


Minireview

Microfluidic devices for studying bacterial taxis, drug testing and biofilm formation

Sandra Pérez-Rodríguez,^{1,2,3} José Manuel García-Aznar^{1,2} and Jesús Gonzalo-Asensio^{3,4,5*} 

¹Aragón Institute of Engineering Research (I3A), Department of Mechanical Engineering, University of Zaragoza, Zaragoza, 50018, Spain.

²Multiscale in Mechanical and Biological Engineering (M2BE), IIS-Aragón, Zaragoza, Spain.

³Grupo de Genética de Micobacterias, Department of Microbiology, Faculty of Medicine, University of Zaragoza, IIS Aragón, Zaragoza, 50009, Spain.

⁴CIBER Enfermedades Respiratorias, Instituto de Salud Carlos III, Madrid, 28029, Spain.

⁵Institute for Biocomputation and Physics of Complex Systems (BIFI), Zaragoza, 50018, Spain.

Summary

Some bacteria have coevolved to establish symbiotic or pathogenic relationships with plants, animals or humans. With human association, the bacteria can cause a variety of diseases. Thus, understanding bacterial phenotypes at the single-cell level is essential to develop beneficial applications. Traditional microbiological techniques have provided great knowledge about these organisms; however, they have also shown limitations, such as difficulties in culturing some bacteria, the heterogeneity of bacterial populations or difficulties in recreating some physical or biological conditions. Microfluidics is an emerging technique that complements current biological assays. Since microfluidics works with micrometric volumes, it allows fine-tuning control of the test conditions. Moreover, it allows the recruitment

of three-dimensional (3D) conditions, in which several processes can be integrated and gradients can be generated, thus imitating physiological 3D environments. Here, we review some key microfluidic-based studies describing the effects of different microenvironmental conditions on bacterial response, biofilm formation and antimicrobial resistance. For this aim, we present different studies classified into six groups according to the design of the microfluidic device: (i) linear channels, (ii) mixing channels, (iii) multiple floors, (iv) porous devices, (v) topographic devices and (vi) droplet microfluidics. Hence, we highlight the potential and possibilities of using microfluidic-based technology to study bacterial phenotypes in comparison with traditional methodologies.

Introduction

Bacteria are microscopic organisms that inhabit all known habitats on Earth, either interacting with natural environments or leading to beneficial or harmful effects in specific hosts. For instance, some environmental bacteria grow attached to plants, and a relationship is created between both entities. Usually, this is established as a symbiotic interaction, in which nutrients and protection are provided (Backer *et al.*, 2018; Vives-Peris *et al.*, 2020), but some studies have described non-symbiotic relationships between plants and bacteria (Lamouche *et al.*, 2018; Deng *et al.*, 2020). This kind of positive relationship has also been established between bacteria and animals or humans; for example, the formation of the intestinal microbiota that facilitates digestion, outcompetes pathogenic microorganisms and provides essential nutrients (Debré and Gall, 2014). In this context, research on the beneficial relationship between the microbiota and the human host has resulted in biotechnological applications, such as probiotic bacteria, which contribute to maintaining human health by battling harmful microorganisms, healing gut and skin tissue or strengthening the epithelial barrier (Lukic *et al.*, 2017). On the other hand, some pathogenic bacteria have evolved to cause disease, either by producing virulence

Received 9 July, 2020; revised 1 February, 2021; accepted 2 February, 2021.

*For correspondence. E-mail jagonzal@unizar.es; Tel. +34 976762420; Fax +34 976762604.

Microbial Biotechnology (2022) 15(2), 395–414

doi:10.1111/1751-7915.13775

Funding information

This work was supported by the Spanish Ministry of Education, Culture and Sport (FPU grant: FPU16/04398) to S. P.-R.; the Spanish Ministry of Science, Innovation and Universities (RTI2018-094494-B-C21) to J. M. G. A. and the Spanish Ministry of Science and Innovation (PID2019-104690RB-I00) to J. G.-A.

© 2021 The Authors. *Microbial Biotechnology* published by John Wiley & Sons Ltd and Society for Applied Microbiology.

This is an open access article under the terms of the Creative Commons Attribution-NonCommercial License, which permits use, distribution and reproduction in any medium, provided the original work is properly cited and is not used for commercial purposes.

factors, developing mechanisms to survive in unfavourable environments or by manipulating the host immune system, among others (Kudva *et al.*, 2016; Johnson, 2018). Even though our in-depth knowledge of pathogens has led to vaccine and antibiotic development to treat many infectious diseases (Henriques-Normark and Normark, 2014), additional research is needed to cope with the emerging threat of antimicrobial resistance, emerging and neglected infectious diseases and research into fastidious pathogens.

Understanding bacterial interactions with cells under physiological conditions is essential to study certain bacterial phenotypes. Traditional microbiological *in vitro* techniques include microscopy, cell infection models and recent molecular, cellular and immunological assays (Houpikian and Raoult, 2002; Balouiri *et al.*, 2016). These methods have provided and continue to provide inestimable information, contributing to gaining insight into the molecular and cellular microbiology of the host-bacteria interplay. However, traditional methodologies have some limitations. On the one hand, although culture procedures have improved with time, bacteria still exist that cannot be cultured under *in vitro* conditions (Ito *et al.*, 2019; Bodor *et al.*, 2020). On the other hand, *in vitro* and *ex vivo* models are not able to fully recreate the physiological environment, such as gastric acidity, whose pH increases while digestion occurs (Vinderola *et al.*, 2017). Consequently, *in vitro* and *in vivo* results do not always correlate. In addition, some phenotypes, such as biofilm formation, are traditionally studied under simplistic environments that do not mimic complex physiological scenarios (Lebeaux *et al.*, 2013). Nevertheless, the recent advent of microfluidics can help to solve some of these limitations, to not only advance fundamental microbiological research but also help in the development of therapeutic interventions.

Microfluidics is known as the technique that handles microscale fluid flows (Sackmann *et al.*, 2014), allowing the integration, miniaturization and automation of several processes (Halldorsson *et al.*, 2015). Working with manufactured microdevices involves the use of small volumes (on the microliter scale), assuring better control of environmental conditions and saving reagents, biological material, residues and space (Shin *et al.*, 2012). However, the main advantage of these microfluidic devices is the possibility of recreating biological environments more realistically than traditional macroscopic cultures in flasks, well plates or dishes (Halldorsson *et al.*, 2015). This approximation can be implemented by three-dimensional cultures of microorganisms embedded in hydrogels that simulate the extracellular matrix or by introducing a flow to mimic interstitial fluid flow that transports nutrients and other microorganisms (Huang *et al.*, 2010). In addition, the physical (rigidity, pressure

forces, fluid flows, etc.) and chemical (pH, attraction and repulsion factors, etc.) conditions can be modified to study adaptations to the changing environment (Velve-Casquillas *et al.*, 2010).

The materials used in the pioneering microfluidic devices were silicon and glass. Nevertheless, the opacity of silicon makes it incompatible with microscopy studies. Moreover, both glass and silicon are characterized by their fragility, difficult bonding protocols and high cost. Altogether, their use has been limited, paving the way for the use of new materials (Sackmann *et al.*, 2014). Since the 1990s, the most utilized material has been polydimethylsiloxane (PDMS), a mineral-organic polymer from the siloxane family (Friend and Yeo, 2010). PDMS presents numerous beneficial properties: optical transparency, gas permeability, flexibility, chemical inertness, biocompatibility, ease of bonding and unbonding to other materials, the possibility of making its surface more hydrophilic and low cost (Weibel *et al.*, 2007). Thus, PDMS has been considered a great candidate for microfluidics studies. Other materials used for this application are thermoplastics, paper and wax (Sackmann *et al.*, 2014).




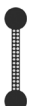


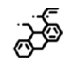






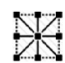
Microfluidic devices have great versatility in terms of design depending on the field of study in which they are applied. The diverse patterns found in the literature have been divided into six groups throughout this review: (i) devices with linear channels, subdividing for one, two and three parallel channels; (ii) devices with mixing channels; (iii) devices with multiple floors; (iv) porous devices; (v) topographic devices and (vi) droplet microfluidics (Table 1).

Our main objective is to compile diverse studies on bacterial behaviour (Table 1), including taxis processes, which are defined as directed bacterial movement towards or away from an external stimulus or gradient (Krell *et al.*, 2011). Depending on the external stimulus, different taxis can be stimulated. If there is a chemical compound, it is chemotaxis; an oxygen gradient, aerotaxis; a flow current, rheotaxis; a light stimulus, phototaxis; a magnetic field, magnetotaxis; a temperature stimulus, thermotaxis and a pH stimulus, pH taxis. We also included studies in relation with growth assays under different environments, in the presence of diverse compounds and on the formation of biofilms, known as microbial communities established in the self-produced extracellular substances (Mirzaei *et al.*, 2020).

Microfluidic devices with linear channels

Devices with linear channels are the most basic design and consist of straight channels with openings at each end. Multiple channels can be added in parallel to create more versatile devices. In this review, we focused on devices with one, two and three channels.

Table 1. Summary of different articles that used microfluidics-based approaches to study different phenomena. Research topic icons were constructed by Freepik (chemotaxis, aerotaxis, magnetotaxis, pH taxis, growth tests and biofilm formation), Good Ware (rheotaxis) and fps web agency (thermotaxis) from www.flaticon.com.

Linear channels		Cheng <i>et al.</i> (2007), Ahmed and Stocker (2008), Lanning <i>et al.</i> (2008), Roggo <i>et al.</i> (2018)	Kim <i>et al.</i> (2016), Menolascina <i>et al.</i> (2017), Stricker <i>et al.</i> (2019)	Kaya and Koser (2012), Caspi (2014)	Myklatun <i>et al.</i> (2017), Rismani Yazdi <i>et al.</i> (2018b), Miller <i>et al.</i> (2019)	Jeong <i>et al.</i> (2014), Munigesan <i>et al.</i> (2017), Paulick <i>et al.</i> (2017)	Zhuang <i>et al.</i> (2015), Parvinzadeh Gashti <i>et al.</i> (2016)	Balaban <i>et al.</i> (2004), Wang <i>et al.</i> (2010), Aldridge <i>et al.</i> (2012), Lambert and Kussel (2014), Matsumoto <i>et al.</i> (2016), Kim <i>et al.</i> (2019), Li <i>et al.</i> (2019), Simmons <i>et al.</i> (2020)	Jeong <i>et al.</i> (2014)
Mixing channels		Mao <i>et al.</i> (2003), Englert <i>et al.</i> (2009)	Lam <i>et al.</i> (2009), Golchin <i>et al.</i> (2012)						
Multiple floors			Adler <i>et al.</i> (2012)						
Porous devices		Long and Ford (2009), Wright <i>et al.</i> (2014)		Durham <i>et al.</i> (2012), Dehkharghani <i>et al.</i> (2019)				Hyun <i>et al.</i> (2008)	Aufrecht <i>et al.</i> (2019)
Topographic devices				Marcos <i>et al.</i> (2009), Rusconi <i>et al.</i> (2010), Yazdi and Ardekani (2012), Ishikawa <i>et al.</i> (2014), Marty <i>et al.</i> (2014), Zhang <i>et al.</i> (2019)	Rismani Yazdi <i>et al.</i> (2018a)			Takeuchi <i>et al.</i> (2005), Cho <i>et al.</i> (2007)	Yazdi and Ardekani (2012), Hansen <i>et al.</i> (2016), Rath <i>et al.</i> (2017), Zhang <i>et al.</i> (2019)
Droplet microfluidics									
Chemotaxis									
Aerotaxis									
Rheotaxis									
Magnetotaxis									
Thermotaxis									
pH taxis									
Growth tests									
Biofilm formation									

Single-channel devices

As the name suggests, these devices consist of a unique central channel into which bacteria are introduced. There are two main approximations with this design. On the one hand, a tactic signal gradient can be generated inside the channel. On the other hand, researchers can use several devices so that each device presents a different condition inside the channel. In the first case, bacterial behaviour is analysed along the channel, whereas in the second approximation, bacterial behaviour is compared across different devices.

Chemotaxis was among the pioneering studies carried out on microfluidic devices. Generation of a gradient inside the channel by the addition of a signal molecule on one end and bacteria on the other end allows for observations of chemotactic movements along the channel. The chemotactic response of *Escherichia coli* to aspartate and serine was discovered by the J. Adler laboratory in the 1960s (Adler, 1966, 1973). This line of investigation was continued by several researchers (Segall *et al.*, 1982; Liberman *et al.*, 2004), resulting in a deep characterization and description of the stages and molecules involved in the process. Microfluidic assays using gradients inside channels have been able to reproduce previously published results by traditional methods. For example, Ahmed and Stocker introduced *E. coli* bacteria on one aperture, whereas at the opposite opening, they introduced α -methylaspartate and L-serine as chemoattractants (Fig. 1A). The *E. coli* responded to this chemical gradient, increasing its speed by 35% (Ahmed and Stocker, 2008).

Aerotactic assays were carried out by Stricker *et al.*, who designed a microdevice in which an air bubble was captured in one of the ends, whereas, the rest of the channel was filled with a *Shewanella oneidensis* suspension (Fig. 1B), a facultative anaerobe. This design had two configurations: both openings were closed, or only the end with the bacteria was closed. The oxygen diffused from the bubble to the medium, creating a gradient. Hence, depending on the configuration, the oxygen supply was limited and variable over time or limitless and constant respectively. *S. oneidensis* migrated towards the bubble until it established itself at a point where the oxygen conditions were optimal, maintaining its motility. In the case of limited oxygen, as the bacteria consumed the oxygen, they entered a non-motile vibration state. The authors concluded that the aerobic-anaerobic transition determined the motile and non-motile states of the bacteria (Stricker *et al.*, 2019).

The integration of multiple units on a unique microfluidic platform allows for the study of multiple conditions at the same time. For example, rheotactic and magnetotactic effects on *E. coli* have been analysed using multiple

single channels through which a flow of bacteria passes. Under resting conditions, *E. coli* migrated on circular trajectories; with moderate laminar flow, they migrated in the opposite direction of the flow, and under high flow conditions, the bacteria were dragged in the same direction of flow (Kaya and Koser, 2012). It has also been demonstrated that flow interferes with magnetic stimuli. Miller *et al.* added a magnet on the centre in the middle of the channel and bound *E. coli* to magnetic microbeads (Fig. 1C). In this way, the authors could isolate bacteria by passing them through the channel. They determined that switching the flow has the highest recruitment ratio (Miller *et al.*, 2019). Following a similar strategy, Chen and De La Fuente mimicked the natural environment of *Xylella* by applying a continuous flow in two parallel channels. By increasing the calcium concentration to 2 mM, they confirmed that the twitching speed was significantly increased. In addition, RNA-seq determined that calcium regulated the transcription of genes related to the type IV pili mechanism, pathogenicity and host adaptation (Chen and De La Fuente, 2020).

These devices have also been used to test drug resistance. *Pseudomonas aeruginosa* was cultured inside four independent channels, each containing different dilutions of an antimicrobial compound. The results correlated with standard antimicrobial susceptibility tests and produced results within 3 h. Additionally, by using microfluidics, the authors detected alternative phenotypes linked to the use of some drugs, such as bacterial elongation in the presence of ciprofloxacin or piperacillin or spheroplast and bulge formation in the presence of meropenem (Matsumoto *et al.*, 2016).

Microfluidics offers high flexibility in terms of design, making it suitable for numerous research approaches. Developing smaller channels and adjusting them to the measurements of the studied bacteria (Fig. 1D) allows the capture of bacteria according to their size and shape for identification by electron microscopy and testing of their resistance to antibiotics (Balaban *et al.*, 2004; Li *et al.*, 2019). Moreover, a single bacterium could be trapped to examine its generational growth. Working with *E. coli* under a continuous flow of nutrients that simulates the exponential phase of *in vitro* growth, it was discovered that the division rate of the initial cell remained constant over time, contradicting previous results that indicated the rate decreases (Wang *et al.*, 2010).

Another approach to trap bacteria is by designing small side chambers perpendicular to the central channel where the bacteria are analysed. Multiple *E. coli* were introduced into these lateral chambers to study their adaptative memory mechanisms when carbon nutrients were removed from the central channel. The authors found that *E. coli* presented phenotypic memory by which the bacteria maintained the production of lactose utilization enzymes

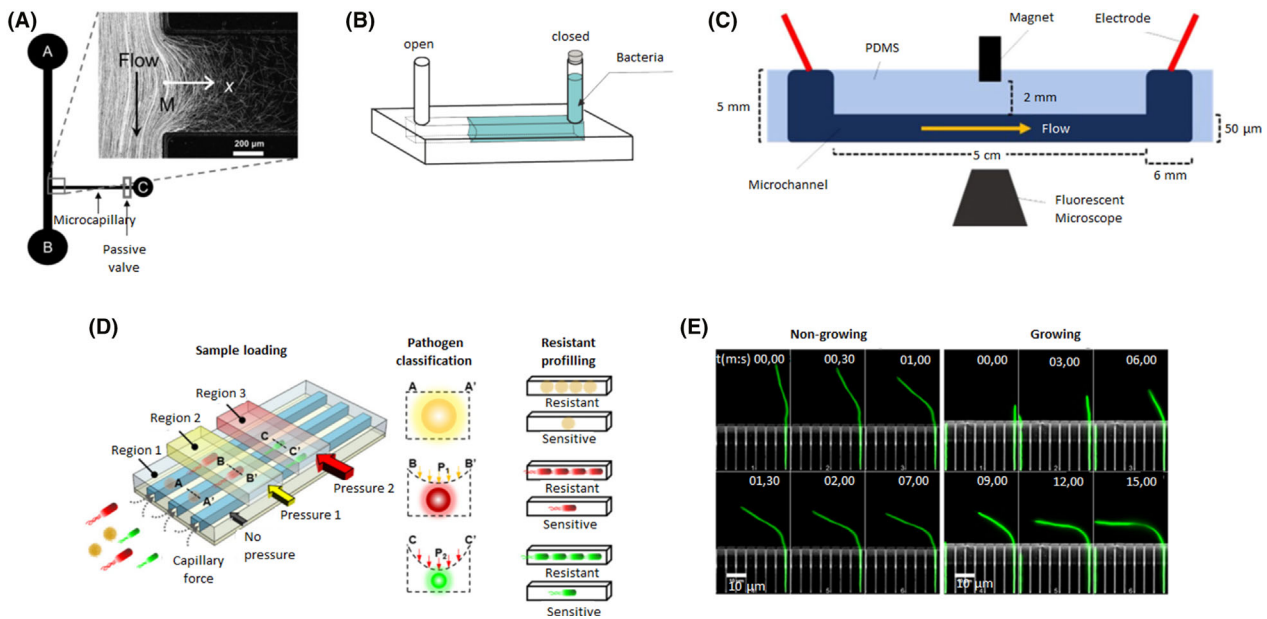


Fig. 1. Microfluidic device designs of individual and linear channels. A. The bacterial flow travelled from reservoir A to B, whereas, chemoattractants were added to reservoir C. A fraction of the bacterial population swam into the capillary where chemotaxis was studied. Adapted from (Ahmed and Stocker, 2008). B. An oxygen gradient was generated by capturing an air bubble on one of the ends of the channel. The opposite end was filled with a bacterial solution. Adapted from (Stricker *et al.*, 2019). C. A magnet was incorporated in the middle of the microfluidic device to attract magnetotactic bacteria that flowed through the channel. Adapted from (Miller *et al.*, 2019). D. A microfluidic device with different regions where pressure could be applied. Depending on the pressure exerted, the channels contracted to different sizes and were able to trap bacteria as a function of their size and shape. Three different bacteria (yellow, red and green) were trapped in regions 1, 2 or 3 (with increasing pressure from 1 to 3). Then, antibiotics were added to examine drug resistance and determine if they were resistant or sensitive. Adapted from (Li *et al.*, 2019). E. A microfluidic device with a side chamber of the same size as the *E. coli* body trapped single bacteria while their flagellum remained freely mobile in the central channel. Hydrodynamic forces were applied to non-growing and growing bacteria (green) to determine their bending force and filament deformation at different times (mm, ss: 00,00–15,00). Adapted from (Caspi, 2014). All figure panels were reproduced/adapted with permission from the corresponding publisher and/or journal. Credits for these figures are provided in the References section of the manuscript.

for ten generations, reducing lag phases in response to switching fluctuations in glucose- or lactose-rich environments. *E. coli* also showed response memory, by which gene expression was maintained after the removal of inducers, promoting bacterial adaptation to short-term changes in the surroundings (Lambert and Kussel, 2014). Single bacteria can also be caught in these side chambers. For instance, Aldridge *et al.* trapped a single *Mycobacterium smegmatis* in each chamber and discovered that these bacteria did not show symmetrical division, instead preferentially elongating their 'old pole'. This results in populations with different sizes and elongation rates, which are affected differently by antibiotics (Aldridge *et al.*, 2012). On the other hand, Caspi drew a chamber size similar to *E. coli* body size, managing to catch bacteria oriented in such a way that their flagellum remained in the central channel (Fig. 1E). By applying hydrodynamic forces through the central channel, bending forces and filament deformation were calculated. At low flow rates ($200 \mu\text{l h}^{-1}$), twice as much force was needed to deform non-growing bacteria to the same extent as growing bacteria. He deduced that this result is due to the difference

between the elastic response of non-growing cells, which could recover their initial conformation when the flow was stopped, in comparison to the plastic-elastic of the growing cells, which were irreversibly deformed (Caspi, 2014).

The interaction of bacteria with bacteriophages was recently studied by Simmons *et al.* in 2020 using linear devices due to the highly controlled conditions offered by microfluidic techniques. *E. coli* was seeded on the microfluidic channel for 48 h with a constant flow to allow biofilm formation. Then, T7 bacteriophages were introduced to infect the bacteria, and biofilm development was analysed for 48 h. Combining their results with computational tools, the authors were able to develop a simulation of the population dynamics of phages that took into account environmental factors such as the ratio of bacterial growth and phage replication, nutrient diffusion or phage susceptibility (Simmons *et al.*, 2020).

Two-channel devices

This kind of chip presents a configuration that is based on two different channels that may or may not be connected.

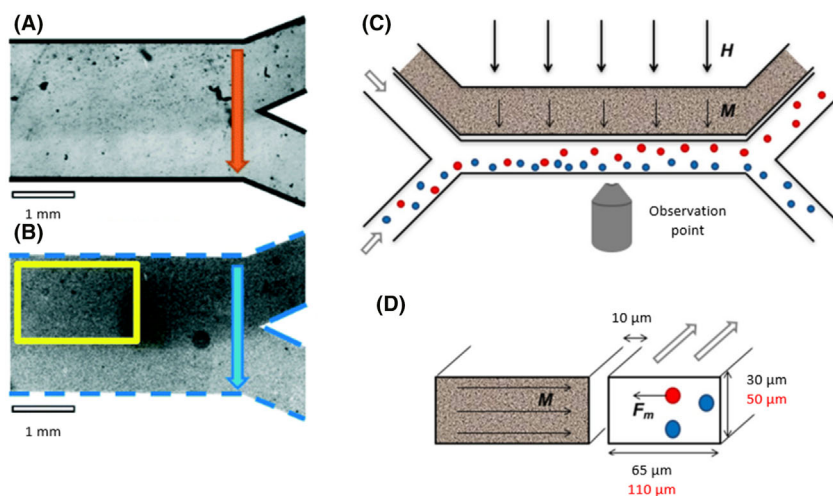


Fig. 2. (A) A Y-shaped microfluidic device with biofilm growth into the upper part of the common channel visualized by bright-field transmission microscopy (A) and radiometric pH imaging (B). Adapted from (Parvinzadeh Gashti *et al.*, 2016). (C) A microfluidic device with two linear channels, in which one contained a ferrofluid (grey channel) and the other channel contained bacteria (white channel). An external magnetic field (H) magnetized the ferrofluid (M), creating a gradient field. Magnetotactic bacteria (red) sensed the magnetic field and suffered an attractive force (F_m), whereas, the nonmagnetic bacteria (blue) were not affected. Longitudinal view (C) and transversal view (D). Adapted from (Myklatun *et al.*, 2017). All figure panels were reproduced/adapted with permission from the corresponding publisher and/or journal. Credits for these figures are provided in the References section of the manuscript.

In the case of being connected, two inputs converge into only one outlet. Lanning and colleagues (2008) used a channel-connected device to introduce bacteria and bacteria with chemoattractants into each inlet to study the response of *E. coli* to α -methylaspartate and aspartate, obtaining results similar to those obtained by traditional methods. Following a similar approach, Gashti *et al.* entered *Streptococcus salivarius* through a single inlet, managing to develop a biofilm only at the upper part of the central channel. This central channel contained fluorescein, a pH indicator that showed a decrease in environmental pH in the biofilm area (Fig. 2A and B). Then, they removed glucose from the medium and observed that the pH returned to physiological conditions in approximately 30 min. However, when glucose was introduced again, the medium acidified within a few minutes to a pH close to 5 (Parvinzadeh Gashti *et al.*, 2016).

If the channels are independent, a different fluid passes through each channel, but each channel has some effect on the other. For instance, if a magnetotactic bacterium, such as *Magnetospirillum gryphiswaldense*, was exposed to an orthogonal magnetic field created by a ferrofluid, the bacteria would be attracted to the channel in which the ferrofluid circulated (Fig. 2C and D; Myklatun *et al.*, 2017).

Three-channel devices

The inclusion of a third channel provides more possibilities because it allows the generation of a gradient in the central channel by adding a signal molecule to a lateral channel,

whereas, the opposite lateral channel maintains the culture conditions and acts as a control. In this way, bacteria are seeded in the central channel, and subsequently, the bacterial movement in response to the gradient can be analysed. *E. coli*, as a model bacterium, has been used in multiple examples to create different gradients and study a wide range of bacterial phenotypes. Chemotactic responses were determined by adding α -methylaspartate, L-serine and aspartate to one channel, generating a chemical gradient (Fig. 3A). It was demonstrated that the strongest migratory response occurred in the presence of L-serine, and the concentrations of α -methylaspartate and aspartate had to be increased to observe significant migration (Cheng *et al.*, 2007; Roggo *et al.*, 2018). The relationship between nutrients and chemotaxis was studied by the incorporation of water channels with different temperatures, creating a profile gradient between 32 and 37°C. *E. coli* are attracted to higher temperatures, so they migrated in that direction. In the first stage, nutrient consumption was higher under those conditions due to an increase in its metabolic activity. Thus, in the second stage, a nutrient gradient was generated, with a higher concentration in cold zones. In this latter stage, the bacteria migrated towards low-temperature areas (Murugesan *et al.*, 2017; Paulick *et al.*, 2017).

In addition to *E. coli*, other bacteria have been studied within these devices. Developing a temperature gradient, Jeong *et al.* established three biofilm formation patterns for Antarctic marine bacteria (Fig. 3B). *Pseudoalteromonas arctica* aggregated at high temperatures, approximately 37–41°C, *Pseudoalteromonas* sp. associated at cold temperatures, 0–18°C,

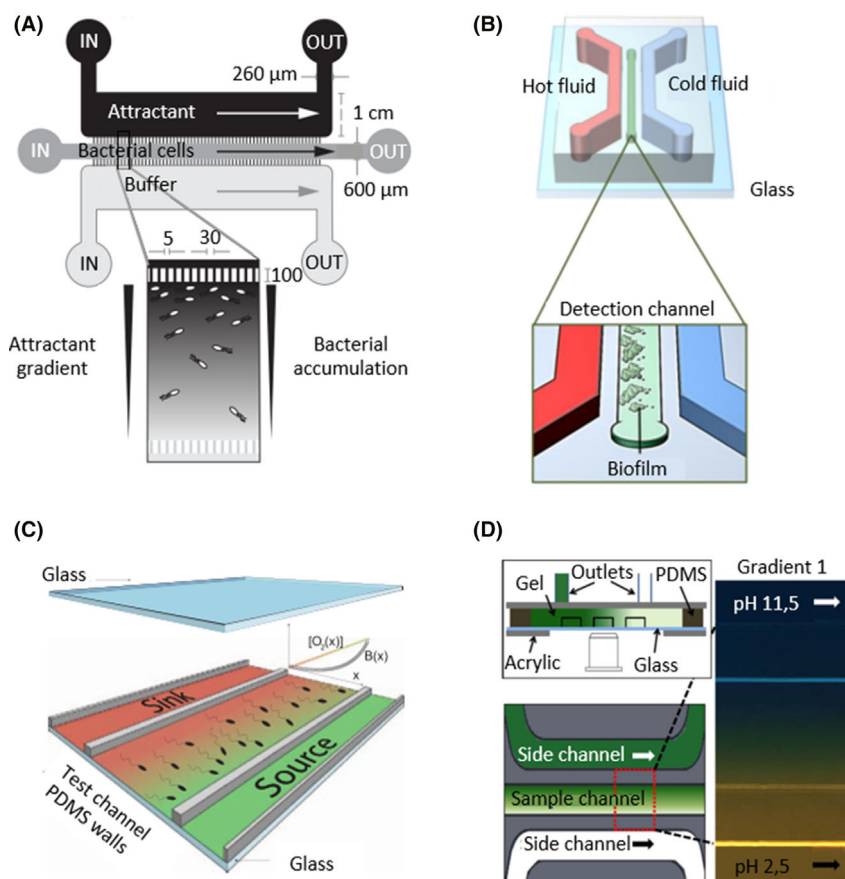


Fig. 3. Microfluidics devices with three channels can generate gradients by adding different conditions to each lateral channel. A. The upper channel was filled with a chemical attractant, and the bottom channel was filled with buffer, generating a chemical gradient in the central channel that was filled with a bacterial solution. Bacterial accumulation was studied in the central channel to determine chemotaxis. Adapted from (Roggo *et al.*, 2018). B. Lateral channels were filled with hot (red) and cold (blue) fluids to generate a thermal gradient in the central channel. Bacteria were seeded on the central channel, and biofilms were closely formed at higher temperatures. Adapted from (Jeong *et al.*, 2014). C. A linear oxygen concentration flowed from the source (green) to the sink (red), creating a gradient in the test channel where the bacterial aerotactic response was analysed. Adapted from (Menolascina *et al.*, 2017). D. Side channels were filled with solutions with different constant pH values, 11.5 (blue) and 2.5 (yellow), which diffused through the PDMS walls, generating a pH gradient in the sample channel. Adapted from (Zhuang *et al.*, 2015). All figure panels were reproduced/adapted with permission from the corresponding publisher and/or journal. Credits for these figures are provided in the References section of the manuscript.

and biofilm formation of *Shewanella frigidimarina* was not affected by temperature (Jeong *et al.*, 2014). By applying reduced-oxygen media through one lateral channel, the aerotactic responses of *Bacillus subtilis*, *E. coli* and *S. oneidensis*, all of which are facultative anaerobes, were determined (Fig. 3C). While *Bacillus* and *Escherichia* migrated towards the presence of oxygen, *S. oneidensis* migrated to low-oxygen areas (Kim *et al.*, 2016; Menolascina *et al.*, 2017). pH and antibiotic gradients have also been developed within these devices. *Serratia marcescens* was exposed to a pH gradient to establish its optimal pH at 7–7.3 (Fig. 3D; Zhuang *et al.*, 2015), and *P. aeruginosa* was grown in the presence of different drug gradients to quantify its minimum inhibitory concentration (Kim *et al.*, 2019).

Furthermore, microfluidics enables the integration of several stimuli in a single device, allowing the study of different

stimuli competing in one single chip. Rismanu Yazdi *et al.* revealed that the capacity of *Magnetospirillum magneticum* to overcome a current depends on the flow, magnetic field and relative orientation. The bacterium could overcome a flow 2–3 times higher when swimming perpendicular to it. However, if a magnetic field was applied, its magnetotactic response allowed it to overcome the counter direction flow (Rismani Yazdi *et al.*, 2018b).

Microfluidic devices with mixing channels

Microfluidic devices with mixing channels are more complex than those explained above since they require a network of channels, which is challenging in terms of both device design and fabrication. They consist of a series of interconnected microchannels that allow

diffusive mixing. This channel network is used to generate a linear concentration gradient (Fig. 4A) or specific microenvironments whose conditions require precise control (Fig. 4B).

The *E. coli* response to chemical gradients of L-aspartate and nickel(II) ions ($\text{Ni} + 2$) was tested. Bacteria were attracted to low concentrations of L-aspartate and deterred from high concentrations of L-aspartate and $\text{Ni} + 2$. By genetic manipulation, researchers obtained bacteria with knockouts of membrane receptors and flagella proteins, corroborating Adler's discovery (Adler, 1966) that the Tar receptor sensed L-aspartate and $\text{Ni} + 2$ (Mao *et al.*, 2003; Englert *et al.*, 2009). On the other hand, with an oxygen mixture, researchers created different highly controlled aerobic and anaerobic environments to grow several bacteria, such as *E. coli* (facultative anaerobe), *Actinomyces viscosus* (aerobe), *Streptococcus mutans* (anaerobe) and *Fusobacterium nucleatum* (anaerobe). They achieved optimal growth conditions for each bacteria using a differential oxygenator, providing high concentrations of oxygen for aerobic bacteria, low concentrations for facultative anaerobic bacteria and a nitrogen (N_2) flow for obligate anaerobes (Lam *et al.*, 2009; Golchin *et al.*, 2012).

Devices with multiple floors

Different layers of PDMS, with the same or distinct designs, can be successively bonded to create a microfluidic device with more than one floor. This allows the study

of the relationship between two conditions at the same time or to recreate 3D conditions between different tissues. For instance, the development of a circuit of water currents with a temperature gradient located over a layer of PDMS that confined a bacterial suspension allowed the study of the influence of temperature and nutrients on the migration of *E. coli* (Fig. 5A). *E. coli* moved towards hot temperatures until it consumed the nutrients in that area; subsequently, *E. coli* travelled to cold areas where there were still nutrients. Moreover, at high temperatures, the intracellular pH decreased, leading to a drop in their migratory speed (Salman *et al.*, 2006; Demir and Salman, 2012).

Instead of a water circuit, a channel network to generate an oxygen gradient can be bonded to a layer for bacterial culture (Fig. 5B). Adler and colleagues (2012) used this approximation to examine *E. coli* under different aerobic and microaerobic environments, although they discovered no response from the bacterium.

Furthermore, this configuration allows the study of intercellular communication. Jung Kim *et al.* designed a device in which the upper floor consisted of three independent chambers and the bottom floor consisted of a large camera confined by PDMS walls. A permeable membrane that permitted the chemical diffusion of molecules separated the two layers (Fig. 5C). Different bacteria were seeded on the three chambers of the upper floor, and because of the permeable membrane, chemical communication existed between them. Significant differences were observable when bacterial colonies were

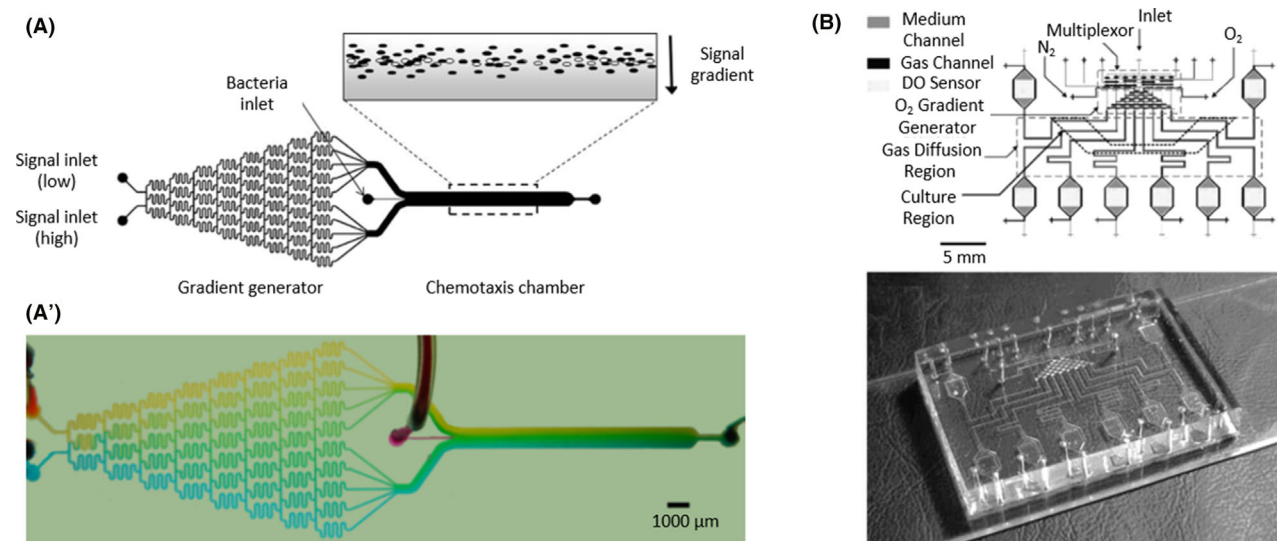


Fig. 4. (A) A microfluidic device with a network of interconnected channels to mix different inlets and generate a highly controlled conditions as an output in the chemotaxis chamber. Live (black ovals) and dead (white ovals) bacteria were introduced in the chemotaxis channel to track migration in response to a signal gradient (grey). (A') Representation of the gradient formation using blue and yellow food dyes, transforming into a range of greens. Adapted from (Englert *et al.*, 2009). (B) A microfluidic device with two layers of PDMS (medium and gas). The medium layer contained a series of channels with a culture region and a density optical sensor (DO sensor). The gas layer consisted of an inlet for each oxygen (O_2) and nitrogen (N_2) and a multiplexor that created an oxygen gradient to grow aerobic and anaerobic bacteria. Adapted from (Lam *et al.*, 2009). All figure panels were reproduced/adapted with permission from the corresponding publisher and/or journal. Credits for these figures are provided in the References section of the manuscript.

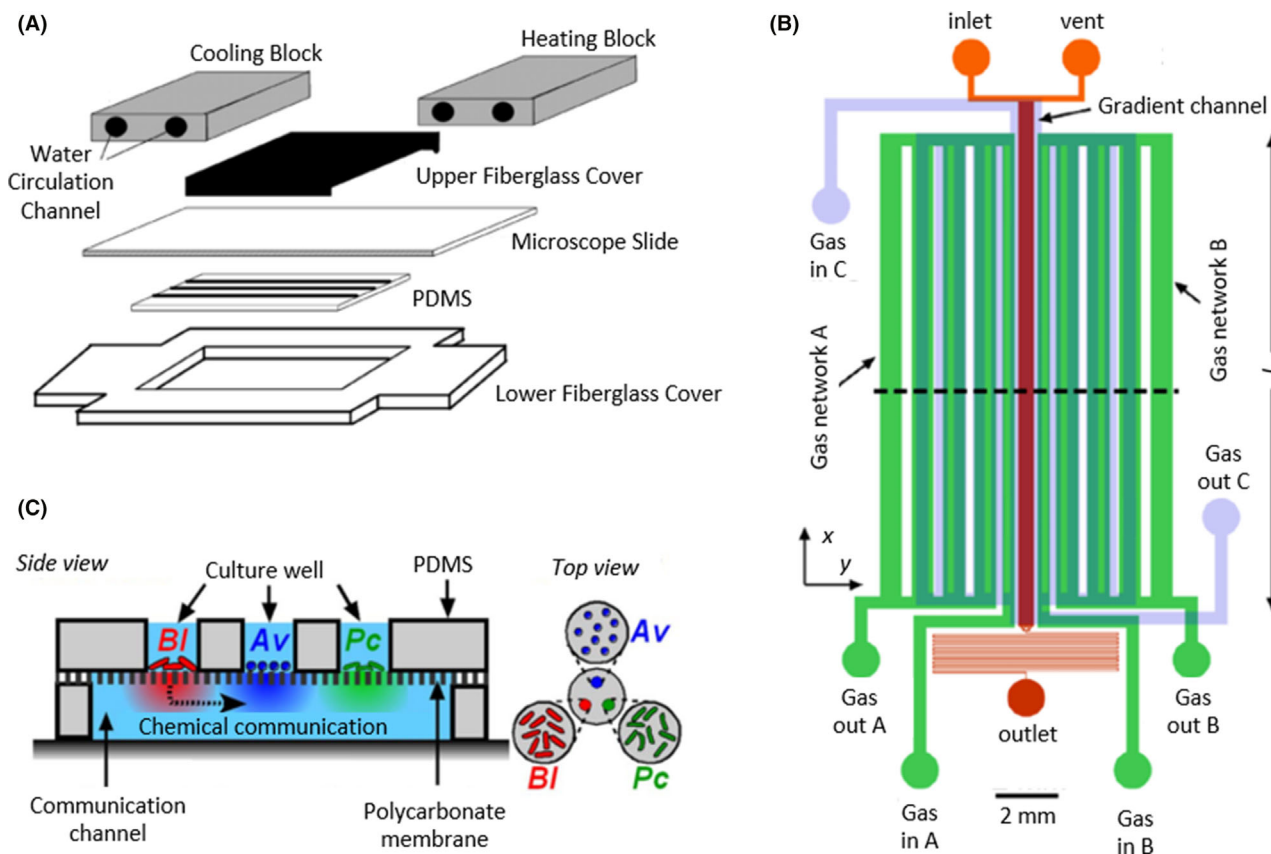


Fig. 5. Microfluidic devices with multiple floors. A. The bottom floor made by PDMS consisted of a camera to grow bacteria and confined by two fiberglass covers, whereas, the upper floor was a water circuit with two blocks, a cooling and a heating block (grey), to create a temperature gradient. Adapted from (Salman *et al.*, 2006). B. Microfluidic device with four floors to control bacterial culture and the oxygen environment: two lower layers, 37 μm and 150 μm deep, were filled with bacterial culture (red and orange), a 150 μm deep layer was a channel circuit for gases A and B (green) and a 340 μm deep layer was a circuit for gas C (blue). Adapted from (Adler *et al.*, 2012). C. Side and top view of a microfluidic device with two layers, one for bacterial culture and the other to allow chemical communication, separated by a polycarbonate permeable membrane. The upper floor consisted of three chambers with three independent bacterial cultures, Av (*Azotobacter vinelandii* in blue), BI (*Bacillus licheniformis* in red) and Pc (*Paenibacillus curdlanolyticus* in green), whose chemicals diffused to the main chamber of the bottom floor. Adapted from (Hyun *et al.*, 2008), copyright (2008) National Academy of Sciences, U. S. A. All figure panels were reproduced/adapted with permission from the corresponding publisher and/or journal. Credits for these figures are provided in the References section of the manuscript.

interrelated or isolated. For example, *Azotobacter vinelandii*, *Bacillus licheniformis* and *Paenibacillus curdlanolyticus* colonies were unstable, and their population size decreased or was maintained at the initial levels over time when grown individually, but when they were connected, these colonies were stable with increasing population sizes. This fact suggested the existence of syntrophic interactions between these bacterial communities (Hyun *et al.*, 2008).

Porous microfluidic devices

The versatility of microfluidics designs permits the use of non-flat surfaces, increasing the scope of studies and allowing the possibility to recreate more realistic environments. For example, porous devices are characterized by a surface full of tiny holes on which bacteria adapt to

grow or migrate. These designs are typically utilized to evaluate chemo- and rheotaxis.

Regarding chemotactic responses, *E. coli* was cultured with an α -methylaspartate gradient, showing higher attraction in porous devices than in plain surfaces. This fact suggested that the flow in porous media increased transverse migration for chemotactic bacteria (Long and Ford, 2009). *Listeria monocytogenes* was also observed in porous devices under acetate gradients (Fig. 6A). *Listeria's* flagella showed changes at acetate concentrations of 10–100 mM, modifying their motility and causing the bacterium to spin (Wright *et al.*, 2014).

If the hole distribution is homogenous (same diameter and same separation distance), the microfluidic device simulates ideal flows in porous surfaces (Fig. 6B). Dehkharghani and colleagues (2019) investigated the dispersion dynamics of *B. subtilis*, noting that hydrodynamic gradients

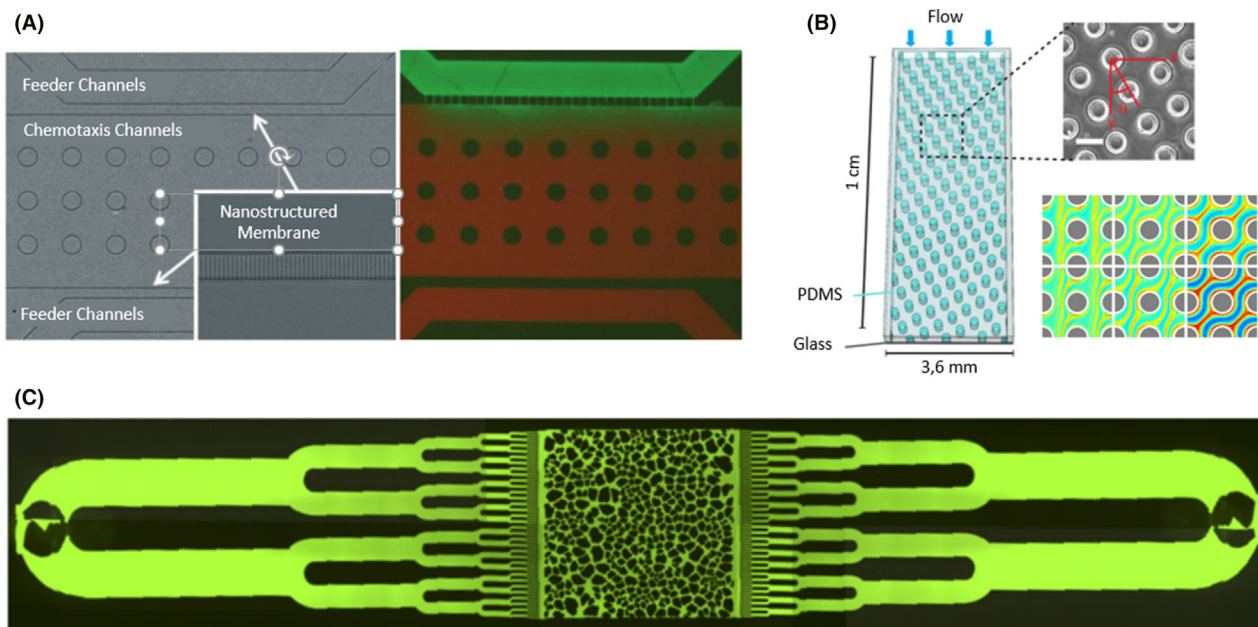


Fig. 6. Microfluidic devices with porous surfaces. A. A porous chemotaxis channel printed 800 nm in diameter and connected with two feeder channels by a nanostructured membrane. To demonstrate that a chemical gradient could be generated within the chemotaxis channel, the fluorescent dyes fluorescein (green) and Texas Red (red) were used to create a colour gradient in the device. Adapted from (Wright *et al.*, 2014). B. A microfluidic device that consisted of a square camera with circular pillars 65 μm in diameter. Blue arrows indicate the direction of bacterial fluid flow, and coloured lines indicate the trajectories of the swimming bacteria. Adapted from (Dehkharghani *et al.*, 2019). C. A microfluidic device with multiple channels that ended on a central camera with a heterogeneous distribution of pores to mimic realistic surroundings, such as soil. Taken from (Aufrecht *et al.*, 2019). All figure panels were reproduced/adapted with permission from the corresponding publisher and/or journal. Credits for these figures are provided in the References section of the manuscript.

hindered transverse bacterial dispersion, promoting dispersion in the same plane and direction as the current.

However, realistic environments are not homogenous, and pore sizes and distances vary. A heterogeneous design recreated soil surroundings, in which the trend of *E. coli* growing faster when close to channels with higher flow was observed (Durham *et al.*, 2012). This approach could also imitate the infiltration of rainwater into soil (Fig. 6C). Aufrecht *et al.* worked with a wild-type *Pantoea* sp. isolated from the rhizosphere and its extracellular polymeric substance (EPS) knockout mutant. No differences were observable between the two strains regarding the growth area. Both tended to choose a preferential route until the accumulated bacteria blocked this route, so the fluid flow redirected to other routes, supplying nutrients to slow-growing bacteria. The only difference noticed between the wild-type and EPS mutant was that the mutant bacteria associated in long chains in the presence of a flow stimulus, whereas, they remained independent in static zones (Aufrecht *et al.*, 2019).

Topographic microfluidic devices

Again applying the design flexibility offered by microfluidics, topographic devices are characterized as showing an irregular design. This could be due to the non-linear

configuration of their channels or the printing of a great variety of patterns on their surfaces. For the first case, we found two different studies in which a single-channel device was developed with streamer shapes (Fig. 7A). Marcos *et al.* used this design to examine rheotaxis on *Leptospira biflexa*, a bacterium from the order Spirochaetales characterized by a spiral shape similar to a helix. Parabolic flow on the non-motile bacterium made it drift perpendicularly to the transverse plane, lining up the helices with the current lines. The alignment direction depended on the chirality of the helices and the velocity of the flow (Marcos *et al.*, 2009). Rusconi *et al.* also worked with this configuration but evaluated *P. aeruginosa* biofilm formation. Bacterial aggregation tended to be the more linear possibility, occupying the centre of the channels and touching only the inner corners, without distinguishing between round or sharp corners (Rusconi *et al.*, 2010).

However, Ishikawa *et al.* designed a streamer-shaped device with different heights. From a linear three-channel device, they modified the height of the central channel, switching two different channels successively. This led to a change in the speed of the flow, affecting the drift movement of *E. coli* from one lateral channel to the other (Ishikawa *et al.*, 2014). Another way that was found to vary the conditions of fluid flow was to print a horseshoe shape in the centre of the channel and trap an air bubble

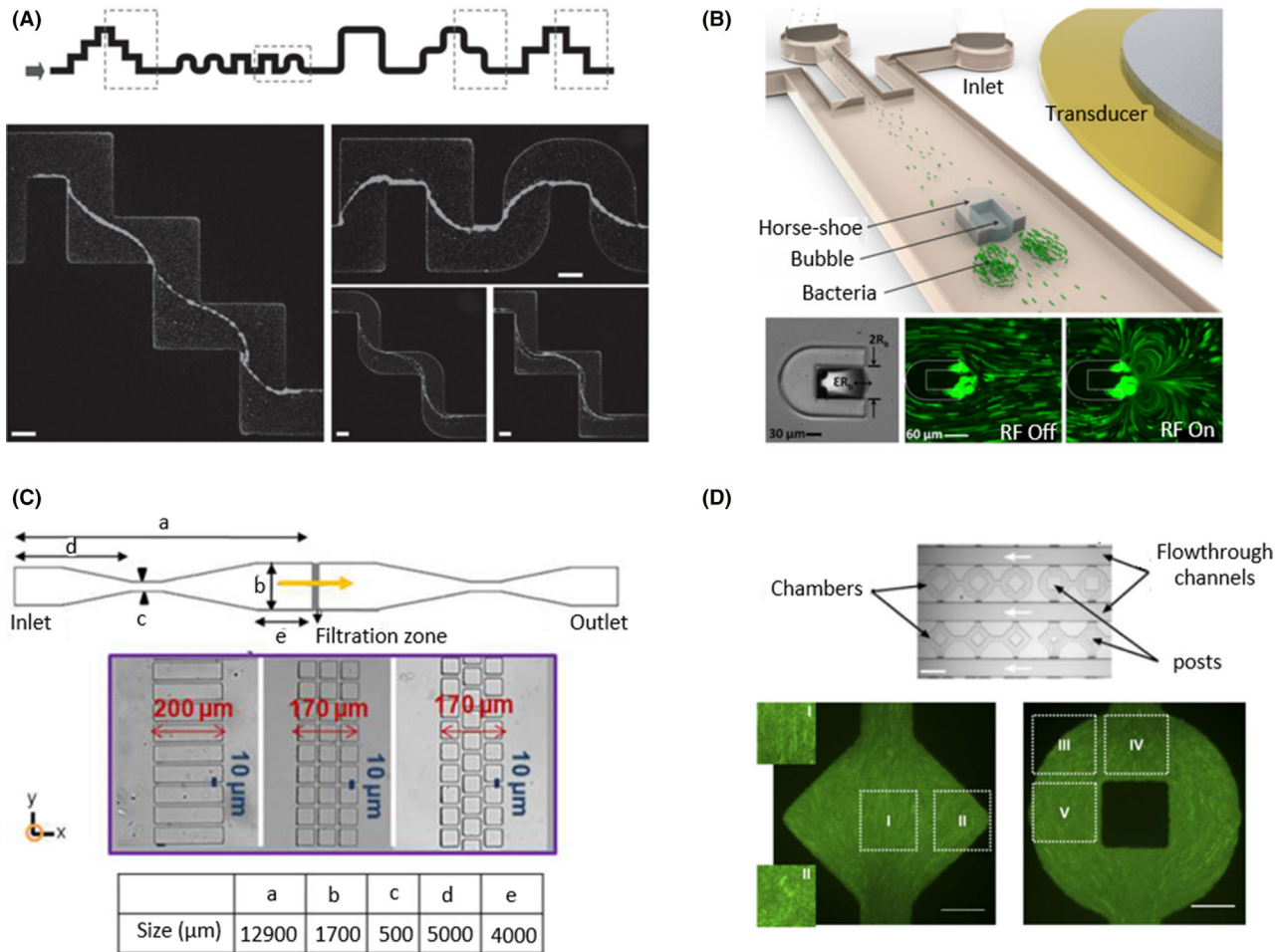


Fig. 7. Topographic microfluidic devices with irregular shapes. A. A single-channel microfluidic device with a streamer shape to examine the formation of biofilms in contact with sharp and rounded corners. Images were taken in the middle horizontal plane after 12 h of a constant flow of $0.75 \mu\text{m}/\text{min}$ (from left to right). Scale bars correspond to $100 \mu\text{m}$. Taken from Rusconi *et al.* (2010). B. A horseshoe shape was printed on the middle of the channel to create a vertical flow in which bacteria were trapped, developing biofilms. The trapped bubble oscillated with an amplitude of εR_b and a diameter of $2R_b$. The vortices were generated by the application of a $1.9 \mu\text{m}$ radio frequency (RF) signal. Green microbeads were used to track trajectories when the transducer was off and of (RF Off/RF On). Adapted from (Yazdi and Ardekani, 2012). C. A linear device with a filtration zone in the centre of the channel with different geometries and distributions of rectangular and square posts. Bacteria were forced to pass through the filtration zone in the direction of the yellow arrow as a recreation of filtration processes. Adapted from (Marty *et al.*, 2014). D. A microfluidic device with geometrical chambers that may include central posts was designed to determine bacterial organization depending on chamber shape. The flow ran through the flowthrough channels in the direction of the white arrows. Bacteria were oriented 90° regions I, II, IV and V and 45° in region III with respect to the x -axis. Scale bars correspond to $50 \mu\text{m}$. Adapted from (Cho *et al.*, 2007). All figure panels were reproduced/adapted with permission from the corresponding publisher and/or journal. Credits for these figures are provided in the References section of the manuscript.

within it (Fig. 7B). By means of acoustic flow of the bubble, a vortical flow was generated, capturing bacteria that formed biofilms after a few minutes (Yazdi and Ardekani, 2012). Zhang *et al.* also caught bacteria to examine *E. coli* biofilm formation. In this case, they added small holes where the bacteria attached and formed biofilms depending on the shear stress applied. Under static conditions or low flow, *E. coli* grew in a planktonic way, whereas under high flow, they grew in communities, forming biofilms (Zhang *et al.*, 2019).

These devices have also been used to observe how bacteria avoid obstacles to move forward. Yazdi *et al.*

printed different flat and curved patterns on the surface of a device. They observed that against curved obstacles, *Magnetospirillum magneticum* maintained its axial direction, whereas when it faced flat obstacles, it switched its direction to backwards until it overcame the obstacle. As *M. magneticum* is a magnetotactic bacterium, researchers evaluated the effects of magnetic fields on the redirection of its migration. Using a microdevice with hexagonal posts, *M. magneticum* showed random migration under resting conditions, but when a magnetic field was applied, the bacteria realigned parallel to the field after interacting with the posts

(Rismani Yazdi *et al.*, 2018a). Following this approach, Marty *et al.* incorporated rectangular and square posts with different distributions to simulate infiltration processes (Fig. 7C). Dead bacteria or inert particles tended to be stuck in the bottleneck area at the top of the posts without going through them. In comparison with the rectangular straight channel distribution, the square connected design presented dead zones with a low flow rate, enhancing the accumulation of bacteria. In addition, the nonaligned square configuration showed tortuous flow areas, in which the flow direction changed, stimulating the formation of colonies (Marty *et al.*, 2014).

The development of non-linear-shaped microfluidic devices could be used to control bacterial shape. Regarding single-cell studies, Takeuchi and colleagues (2005) demonstrated that *E. coli* can grow after adapting itself to the channel shape, such as circle, sinusoidal or zig-zag, and maintain its shape after being released from the channel. Focusing on colonies, Cho *et al.* observed that under high densities, *E. coli* colonies reorganized to propel nutrient transport, enhancing the growth population. Their devices consisted of geometrical chambers that may incorporate a central post (Fig. 7D). The *E. coli* distribution was dependent on the chamber shape (Cho *et al.*, 2007). Hansen *et al.* designed rounded chambers with different diameters, and discovered that *P. aeruginosa* showed better growth in small wells (5–20 µm diameter) than in larger wells (100 µm diameter and beyond). In contrast, *E. coli* formed colonies in wells with a diameter greater than 80 µm. In addition, intercommunity relations were studied with *E. coli* and showed competitive interactions in 40 µm diameter wells but not in smaller pores (Hansen *et al.*, 2016).

Finally, an irregular surface can be an additional material incorporated into the chamber of a microfluidic device, such as a titanium disk, previously treated with an abrasive diamond to generate a uniform pattern where bacteria could attach. Titanium was selected due to its use in medical oral implants. *Streptococcus gordonii*, *Streptococcus oralis*, *Streptococcus salivarius*, *Porphyromonas gingivalis* and *Aggregatibacter actinomycetemcomitans* were grown on titanium disks until the formed biofilms, and their morphology were analysed. *S. gordonii* and *S. salivarius* grew in homogeneous patterns, *S. oralis* demonstrated tower-like structures, *P. gingivalis* formed macrocolonies, and *A. actinomycetemcomitans* showed an open and loose structure (Rath *et al.*, 2017).

Droplet microfluidic devices

Droplet-based microfluidics are characterized for their isolation and confinement of a single bacteria or small populations into individual droplets. These devices include an immiscible two-phase system: an organic

liquid, usually oil, that fills the channel and an aqueous liquid that breaks into droplets when it is introduced into the system (Kaminski *et al.*, 2016). Droplets can be generated by different mechanisms, such as T-junctions, which consist of two inlets that mix the organic and aqueous liquids on the joint (Bai *et al.*, 2016), or flow-focusing geometries that lie in adjustable geometric patterns that allow controlled flow conditions (Lashkaripour *et al.*, 2019). Poisson statistics govern the ratio of organism encapsulation, determining the probability of isolating one or more cells per drop as a function of the starting concentration and occupied fraction of the droplets (Collins *et al.*, 2015).

Droplet-based microfluidics is the most recent and innovative approach among microfluidic devices and shows significant differences in comparison with the previously described designs. On the one hand, droplet-based methodology is still in an optimization phase, with several studies determining the optimal parameters for growing bacteria. On the other hand, although the possibility of generating gradients inside the drop has been demonstrated (Chong *et al.*, 2016), no studies have focused on tactic behaviours. Instead, the predominant assays are oriented to grow tests and biofilm formation. Finally, droplet-based devices introduce the opportunity for the application of some biomolecular techniques.

Regarding optimization studies, static and dynamic cultures have been tested by circulating a constant flow of perfluorinated oil through the main chamber. Oxygen transference was determined by oxygen-sensitive near-infrared luminescence (NIR) measurements, showing a greater rate in dynamic cultures. In addition, the biomass of four bacteria was monitored in both cultures. *B. subtilis* and *Pseudomonas fluorescens*, both obligate aerobes, only grew on dynamic cultures, whereas *E. coli*, a facultative anaerobe, and *Streptomyces aureofaciens*, an aerobe, also grew more in dynamic cultures (Mahler *et al.*, 2015). Continuing the optimization process, Pratt *et al.* examined the stability and size of drops over time by designing a microarray full of parallel channels with connected wells where droplets are stored and then soaking the devices in water-saturated oil. This created conditions in which *P. aeruginosa* could grow for 21.5 h within the drop (Pratt *et al.*, 2019). The *E. coli* standard growth curve in the flask was reproduced using droplet-based microfluidics by trapping drops in a serpentine channel previously sorted by drop size. On both sides of the channel, an electrode was located that simulated an oscillatory effect, supplying a dynamic environment (Ho *et al.*, 2020). Isolation of individual organisms in drops allows the promotion of slow-growing bacteria. By separating these bacteria from fast-growing bacteria that deplete resources, they are prevented from being displaced. Watterson *et al.* isolated bacteria from faecal

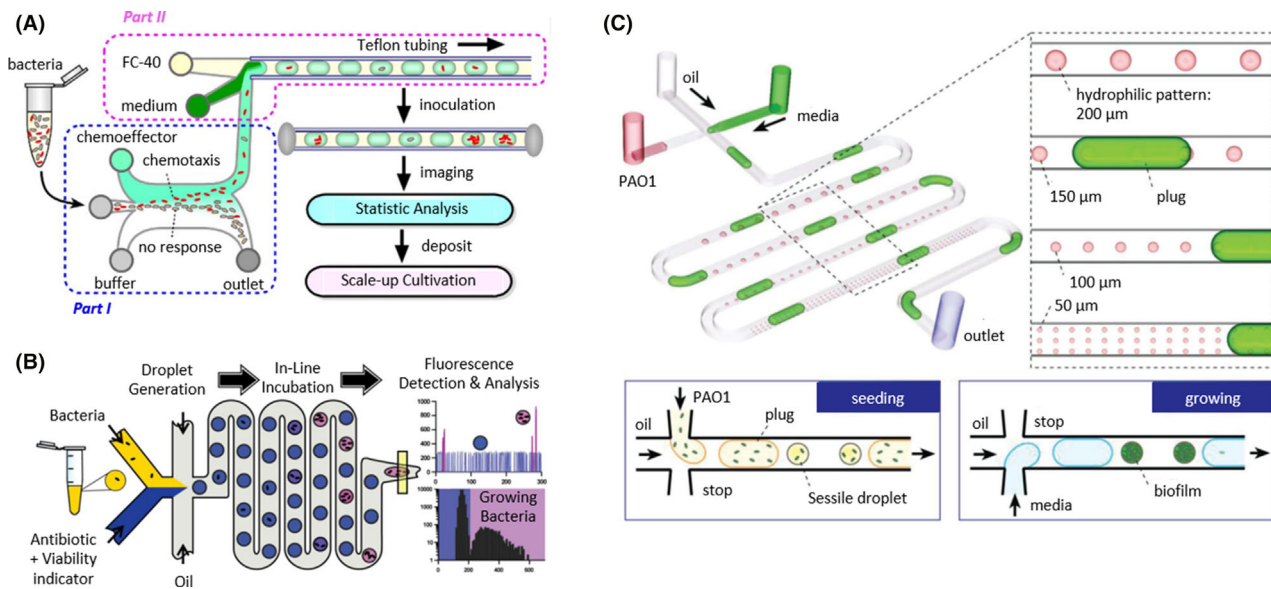


Fig. 8. Droplet-based microfluidic devices. **A.** A microfluidic device divided into two parts. Part I (blue) consisted of three inlets that created an aspartate chemical gradient, allowing the sorting of *E. coli* depending on their chemotactic response. The bacteria that were attracted by aspartate passed through a channel to part II (pink), where droplets were generated by mixing the fluorinated oil FC-40 with medium and bacteria. The droplets were imaged, analysed and cultured. Adapted from (Dong *et al.*, 2016). **B.** Single bacteria were encapsulated in droplets containing antibiotics and a fluorescent viability indicator. Subsequently, there was an in-line incubation that permitted bacterial replication, followed by fluorescence detection in which droplets were either empty (blue circles) or included bacteria (pink circles). Adapted from (Kaushik *et al.*, 2017). **C.** A design starting with a droplet generation system by a T-junction followed by a serpentine with hydrophilic patterns of different sizes where bacteria attached. Biofilm formation was based on two phases. First, there was a seeding process in which *P. aeruginosa* PAO1 was encapsulated and sessile droplets adhered to hydrophilic patterns. The second phase consisted of generating droplets of media to allow bacterial growth until biofilms developed. Adapted from (Jin *et al.*, 2018). All figure panels were reproduced/adapted with permission from the corresponding publisher and/or journal. Credits for these figures are provided in the References section of the manuscript.

microbiota transplants, and by optical density, they selected those that showed slower growth. Genome identification showed the presence of bacteria previously uncultured by traditional methods (Watterson *et al.*, 2020).

As previously mentioned, droplet-based microfluidics studies have not focused on the tactic responses of bacteria. However, Dong *et al.* designed a combined device that consisted of two parts. The first part was similar to a three-channel device where an aspartate chemical gradient was generated to attract and sort fluorescent *E. coli*. Second, a droplet generator encapsulating *E. coli* by the T-junction technique and droplets were analysed as a function of the presence or absence of fluorescence (Fig. 8A). They determined that the *cheZ* gene is essential for the chemotactic ability of *E. coli* (Dong *et al.*, 2016).

Toxicology and antibiotic resistance have been tested in these devices, analysing the growth rates inside drops. *Streptomyces acidiscabies* and *Psychrobacillus psychrodurans*, bacteria that are resistant to heavy metal ions, were exposed to Cu^{2+} , and their dissolved oxygen consumption and cellular density were monitored. Although oxygen consumption decreased in the presence of 0.5 mM Cu^{2+} , it was not completely inhibited,

confirming that these bacteria were resistant to metallic ions (Cao *et al.*, 2015). Kaushik *et al.* designed a device to determine antibiotic effects on bacteria. It consisted of two inlets to generate drops with a single bacterium, followed by a serpentine where bacteria reproduced a couple of times and a camera for fluorescence detection at the end (Fig. 8B). Resazurin was used as a growth reporter because it is reduced by the intracellular electron receptors NADH and FADH and converted into fluorescent resorufin. Through fluorescence analysis, the droplets were characterized as positive or negative depending on the presence or absence of bacteria respectively. *E. coli* was tested with $4 \mu\text{g ml}^{-1}$ gentamycin, and the positive droplet ratio significantly decreased (Kaushik *et al.*, 2017). Bacteria can also be used as reporters to detect antimicrobial compounds secreted by other organisms. Environmental microbes were isolated, and fluorescent *E. coli* and *B. subtilis*, gram-positive and gram-negative bacteria, respectively, were introduced into the droplets. As a function of fluorescence intensity, it was possible to determine the presence of antimicrobial molecules. Afterwards, the organisms are sequenced and identified (Mahler *et al.*, 2019). Unlike traditional methods that require several

experimental steps, these platforms integrate droplet formation, bacterial incubation and growth detection in an uninterrupted system.

Biofilm formation has been studied inside droplets using *B. subtilis* as a model bacterium. It was described that these bacteria first swam individually, started to aggregate in 12 h around the drop edges, and finally sporulated in 48 or 72 h (Chang *et al.*, 2015). Bacteria can also be attached to hydrophilic patterns to grow biofilms adherent to surfaces. *P. aeruginosa* droplets were generated and passed through a channel where they became affixed to circle patterns. Subsequently, a media flow was introduced to allow bacterial growth until the biofilms developed (Fig. 8C). In comparison with the microfluidic devices previously described, this approach eliminated corner effects and avoided channel plugs (Jin *et al.*, 2018). Biofilms have also been formed around oil droplets to study the interactions between bacteria and oil molecules that usually appear in flow environments. *Alcanivorax* aggregated in a wrinkly formation surrounding the drop, *Marinobacter* biofilms were oriented $\pm 45^\circ$ from the leading stagnation point with 50 μm thickness, and *Pseudomonas* formed a tail that dispersed in 14 h (White *et al.*, 2019).

Biomolecular techniques have been applied within this system, mainly in order to detect the presence of bacteria in samples. For example, using fluorescent antibodies against *Salmonella enterica* serovar *typhimurium* in freshcut produce water allowed the detection of contamination and avoided foodborne contamination (Harmon *et al.*, 2020). Fluorescence resonance energy transfer (FRET) based on RNA has also been used to analyse samples. When a droplet contained bacteria-secreted RNases, they cleaved RNA and generated fluorescence (Ota *et al.*, 2019). These devices also allowed sequencing of the complete genome of isolated bacteria and were able to identify soil bacteria uncultured by traditional methods (Hosokawa *et al.*, 2017).

Advantages and disadvantages of microfluidics compared to traditional methods

Microfluidics is a versatile technique that is gaining momentum in the field of microbiological research. The reproducibility of results previously obtained by traditional methods provides confidence and robustness to this tool. A clear example of this fact is the migration assays in which the chemotactic response of *E. coli* to different compounds is studied. Traditional methods are based on inoculating bacteria onto agar plates to analyse the kinetics of colony formation over time. The chemoattractant may be contained in the agar plate itself or may have been used to pre-treat the bacterial sample following the method proposed by Adler (1973). This

method consists of introducing a capillary with chemoattractant into a bacterial solution that is subsequently deposited on an agar plate, and after its incubation, the number of colonies is quantified. By means of this methodology, Mesibov and Adler (1972) demonstrated that *E. coli* was attracted to several amino acids, including L-aspartate, showing a peak at a concentration of 10 mM. Wolfe and Berg used the strategy of incorporating L-aspartate into agar plates and determined that *E. coli* shows maximum attraction at 10 μM (Wolfe and Berg, 1989). On the other hand, through the individual monitoring of bacteria grown in microcapillaries, both Roggo's and Cheng's teams corroborated the attraction of *E. coli* to L-aspartate at such concentrations, also highlighting migratory responses at intermediate concentrations such as 0.1 and 1 mM (Cheng *et al.*, 2007; Roggo *et al.*, 2018). Thus, the similarity and reproducibility of the results obtained by both methods make microfluidics a reliable tool.

However, although both methods are capable of determining optimal concentrations of chemoattractant, agar methods have limitations, such as the impossibility of calculating migration rates. This calculation is unfeasible since individual cells cannot be followed; instead, colony growth is evaluated. Partridge *et al.* decided to transfer colonies on agar plates to liquid cultures. They inoculated part of the cultures in small crystal chambers in order to monitor the bacteria individually, determining a migration speed of approximately 20–25 $\mu\text{m s}^{-1}$ (Partridge *et al.*, 2019). Nevertheless, this approach is incompatible with the generation of chemical gradients. Therefore, it was necessary to rely on microfluidic techniques, such as a single-channel device designed by Ahmed and Stocker, with which they created gradients of α -methylaspartate in a range of concentrations between 0.1 and 1 mM and obtained migration speeds between 0.6 and 13.8 $\mu\text{m s}^{-1}$ (Ahmed and Stocker, 2008).

While traditional methods are limited to working on flat 2D surfaces, such as culture flasks, Petri dishes or well plates, microfluidics offers a new variety of materials with promising properties, among which PDMS stands out. Due to its biocompatibility and gas permeability, it is ideal for cellular and microbiological cultures, but in addition, its optical transparency allows visualization and analysis by microscopy. However, its major advantage is the possibility of combining it with other materials, resulting in great versatility in device design. Thus, microfluidics offers the option of working in heterogeneous or even three-dimensional conditions, on which different stimuli, such as fluid flow or tactic gradients, can be applied. This advantage in culture conditions has been exposed by comparing two strategies to grow bacteria. On the one hand, following a traditional method, Bible

and colleagues (2016) isolated *Pantoea* sp. from the rhizosphere of *Populus deltoides* and grew it on an agar plate. On the other hand, Aufrecht *et al.*, after isolating *Pantoea* sp., cultured it on a surface with heterogeneous pores that simulate a more realistic soil distribution (Aufrecht *et al.*, 2019). In addition, Aufrecht applied a flow stream over the system to recreate rainwater filtration. While *Pantoea* sp. grew homogeneously on the agar plate and formed colonies (Bible *et al.*, 2016), in the microfluidic device, it tended to grow by selecting preferential routes depending on the availability of nutrients provided by the stream flows (Aufrecht *et al.*, 2019). Altogether, it is tempting to conclude that microfluidics offers the possibility of replicating more realistic environments than those offered by traditional methods.

The difference in volume and bacterial numbers used in microfluidics as opposed to conventional methods is also an aspect to consider. Microfluidics uses volumes in the microliter range, while traditional methods usually use volumes in the millilitre range. This small size turns microfluidic devices into portable tools and offers a number of advantages, such as economic savings in reagents, materials and space or a more accurate control of the biological and physical conditions of the study. From a biological perspective, macroscopic cultures contain a high number of bacteria, in the thousands or millions, giving rise to inevitable heterogeneity in the study population. In microfluidic assays, the number of bacteria is reduced to hundreds or even individual bacteria, achieving results that are more precise on the single-cell scale. In the physical environment, specific conditions can be achieved, making the growth of several bacteria possible, including oligotrophic bacteria, which are still a challenge for traditional two-dimensional cultures (Overmann *et al.*, 2017). In addition, microfluidics allows almost instantaneous changes in environmental conditions within the device, allowing the study of bacterial adaptation. Lambert and Kussel designed a microfluidic device composed of a central channel and lateral culture chambers of 25 μm^3 . By adding a flow current through the main channel, they were able to generate transitions in the media conditions in less than 250 milliseconds. As a result, they studied the adaptive response of *E. coli* to fluctuating changes in glucose- or lactose-enriched broth media on a time scale of 1 to 10 generations (Lambert and Kussel, 2014). On the other hand, Phillips *et al.* studied the same adaptive response in 1 ml of *E. coli* cultures, making daily inoculations to perform the media changes. They conducted these experiments over approximately 3000 generations (Phillips *et al.*, 2016). In this way, the greater control over the studied condition results is reflected in the reduced duration of the experiments.

Experimental times can also be shortened by integrating several experimental processes into a single

platform, thus also reducing the number of manipulations by researchers and therefore the risk of contamination and technical variability (Halldorsson *et al.*, 2015). A clear example of the power of integration from microfluidics is droplet-based devices. This can be demonstrated by comparing the approach of these devices to traditional methods in the study of antimicrobial susceptibility. In 1966, the antibiotic susceptibility test was established by means of the standardized disk diffusion method (Bauer *et al.*, 1966), colloquially named the antibiogram, which is still used today (Kibret and Abera, 2011). This method consists of inoculating a bacterial culture onto an agar plate and placing it on a paper disk containing antibiotics that radially diffuse in the agar. After an incubation period, in the case where the bacteria are susceptible to the antibiotic, a growth inhibition zone appears whose diameter correlates with the antimicrobial power of the antibiotic tested. Kaushik *et al.* proposed a droplet-based microfluidic device in which they integrated the incubation of the bacteria in contact with the antibiotic in microdrops with the detection and analysis of its susceptibility (Fig. 8B) through the fluorescence produced by resazurin when reduced by the bacterial metabolic activity (Kaushik *et al.*, 2017). While the standardized method requires several manipulations, including inoculation, deposition of the antibiotic disk or measurement of the diameter of the inhibition zone, the microfluidic device integrates all steps in a continuous flow system where the only manipulation is the initial load of the components to be studied. In addition, the antibiogram requires at least 24 h of incubation, while microfluidic devices allow testing of antimicrobial susceptibility after 1 h. Undoubtedly, this time-saving and minimal technical manipulation are valuable considerations for the use of microfluidic devices in a clinical context, where proper treatment of infected patients requires reliable and instant results.

Nevertheless, microfluidics still has a long way to go to overcome several of the challenges it presents. For example, despite the numerous advantages described above for PDMS, we also have also found some drawbacks. Its major limitation in the cellular field is its capacity to absorb small hydrophobic molecules or biomolecules, such as proteins, interfering with the results of the assays. This demonstration was performed by van Meer *et al.*, comparing the absorption of four cardiac drugs when incubated in standard tissue culture grade polystyrene (TCPS) 96-well and PDMS wells. While the adsorption in the TCPS wells was negligible, PDMS adsorbed between 20% and 80% of the compounds within 3 h (van Meer *et al.*, 2017). PDMS is a porous material that not only absorbs molecules but also allows the passage of organic solvents that can modify the dimensions of the channels. Dangla and colleagues (2010) observed that when filling 50 μm -high

channels with the solvent hexadecane, the channels were deformed by sinking the ceiling parabolically by approximately 7 μm . As a result, protocols are being developed that modify the surface of PDMS to avoid these phenomena (Shin *et al.*, 2018; Gökaltun *et al.*, 2019; You *et al.*, 2020).

Due to its recent appearance, the absence of standardized protocols in microfluidics-based research is evident. Bacteria are mainly visualized using microscopy techniques, which require reporter-labelled bacteria and/or specialized microscopy facilities (Subramanian *et al.*, 2020). This restricts microfluidics assays to visual analysis and model microorganisms, which frequently do not reflect the virulent traits of pathogenic species. The assays carried out are mostly focused on the study of migration trajectories and growth rates, and it is clear that there is a lack of molecular characterization. The development of devices based on droplets has led to a great advance in this field, giving the possibility of studying bacteria at a single-cell level. In addition, some protocols for the extraction of nucleic acids and proteins from samples confined within microfluidic devices have been published (Schilling *et al.*, 2002; Oblath *et al.*, 2013; Julich *et al.*, 2016; Hosokawa *et al.*, 2017). Nevertheless, microfluidics is far from assessing molecular changes at the intracellular level, and new techniques have to be improved to allow genomic, transcriptomic, proteomic and metabolomic research at the same level as established methods. Once these limitations are overcome, microfluidics might become an indispensable technique for research and commercial applications.

Future directions

Most microfluidic studies involving bacteria have been performed using environmental or non-pathogenic species. This fact shows a knowledge gap in the biomedical field regarding the interaction between host cells and bacteria, both symbiotic and pathogenic. A key limitation to study pathogenic species by microfluidic devices is the requirement for specialized time-lapse microscopy facilities within biosafety laboratories. Although this limitation could be partially overcome by using non-pathogenic but phylogenetically related microorganisms, the application of microfluidics for antimicrobial testing or immunological research still requires the presence of pathogenic counterparts.

Some researchers have developed more complex microfluidic devices, integrating several tissues to mimic organs, which is known as organ-on-a-chip. Some of the organs that have been simulated thanks to microfluidics are the gut (Kim and Ingber, 2013), lung (Huh, 2015), liver (Ho *et al.*, 2006), endothelial vessels (Polacheck *et al.*, 2019) and brain (Bang *et al.*, 2019). The

application of bacteria in these systems would not only result in a more complete and realistic approach to recreate complex bacterial interactions with some human organs, such as the intestinal microbiota, but would also allow for a more detailed study of the host-bacterial interplay *in vitro*. A recent example of the potential of this combination is the work of Thacker *et al.*, which includes *Mycobacterium tuberculosis* within a lung-on-a-chip. This device consisted of two monolayers of endothelial and epithelial cells adhered to a porous membrane, recreating the alveolar surface, with a flow of macrophages and *M. tuberculosis* to simulate part of the immune system. They discovered the importance of the surfactant on *M. tuberculosis* infections, since its deficiency led to uncontrolled bacterial growth and its presence is involved in attenuating bacterial virulence (Thacker *et al.*, 2020). This later work involving a deadly pathogen and a lung-on-a-chip device opens attractive perspectives for microfluidics in biomedical applications.

Finally, some molecular biology applications can be adapted to a microfluidic platform allowing high-throughput studies. Specifically, a microfluidic device designed by Mathai *et al.* allows performing multiple quantitative PCR in a single run. This system was successfully applied to decipher the microbial content in complex samples, and constitutes an interesting adaptation of laboratory-level techniques to a microfluidic scale (Mathai *et al.*, 2019).

Conclusions

Throughout this review, we have analysed the potential of microfluidics in the microbiological field. Its great versatility in terms of design allows the recreation of 3D microenvironments, which otherwise allows a more realistic study of certain bacterial phenotypes than traditional methods. As a result, microfluidic devices can reproduce different scenarios, including physical, chemical or biological variations that exist in natural environments. For example, the simplest devices consisting of linear channels have been used to track bacterial migration in response to tactic stimuli, analyse bacterial sensitivity to drugs or study biofilm formation. More complex chips include mixing channels or those with more than one floor that allow greater control of conditions within the channels and/or the co-culture of various species of bacteria. In addition, the surfaces of these devices can be modified to fabricate non-flat channels, resulting in porous devices or topographic devices that recreate natural environments, such as soil, or obstacles with specific shapes. Finally, droplet-based microfluidic devices isolate bacteria on microdroplets, allowing single-cell studies mainly focused on testing drug resistance and biofilm

formation. Together, microfluidics offers versatile approaches to study multiple microbiological scenarios.

Acknowledgements

This work was supported by the Spanish Ministry of Education, Culture and Sport (FPU grant: FPU16/04398) to S. P.-R.; the Spanish Ministry of Science, Innovation and Universities (RTI2018-094494-B-C21) to J. M. G. A. and the Spanish Ministry of Science and Innovation (PID2019-104690RB-I00) to J. G.-A.

Conflict of interest

The authors declare that there is no conflict of interest.

References

- Adler, J. (1966) Chemotaxis in bacteria. *Science* **153**: 708–716.
- Adler, J. (1973) A method for measuring chemotaxis and use of the method to determine optimum conditions for chemotaxis by *Escherichia coli*. *J Gen Microbiol* **74**: 77–91.
- Adler, M., Erickstad, M., Gutierrez, E., and Groisman, A. (2012) Studies of bacterial aerotaxis in a microfluidic device. *Lab Chip* **12**: 4835–4847.
- Ahmed, T., and Stocker, R. (2008) Experimental verification of the behavioral foundation of bacterial transport parameters using microfluidics. *Biophys J* **95**: 4481–4493.
- Aldridge, B.B., Fernandez-Suarez, M., Heller, D., Ambra-vaneswaran, V., Irimia, D., Toner, M., and Fortune, S.M. (2012) Asymmetry and aging of mycobacterial cells lead to variable growth and antibiotic susceptibility. *Science* **335**: 100–104.
- Aufrecht, J.A., Fowlkes, J.D., Bible, A.N., Morrell-Falvey, J., Doktycz, M.J., and Retterer, S.T. (2019) Pore-scale hydrodynamics influence the spatial evolution of bacterial biofilms in a microfluidic porous network. *PLoS One* **14**: 1–17.
- Backer, R., Rokem, J.S., Ilangumaran, G., Lamont, J., Praslickova, D., Ricci, E., *et al.* (2018) Plant growth-promoting rhizobacteria: context, mechanisms of action, and roadmap to commercialization of biostimulants for sustainable agriculture. *Front Plant Sci* **871**: 1–17.
- Bai, L., Fu, Y., Zhao, S., and Cheng, Y. (2016) Droplet formation in a microfluidic T-junction involving highly viscous fluid systems. *Chem Eng Sci* **145**: 141–148.
- Balaban, N.Q., Merrin, J., Chait, R., Kowalik, L., and Leibler, S. (2004) Bacterial persistence as a phenotypic switch. *Science* **305**: 1622–1625.
- Balouri, M., Sadiki, M., and Ibensouda, S.K. (2016) Methods for in vitro evaluating antimicrobial activity: a review. *J Pharm Anal* **6**: 71–79.
- Bang, S., Jeong, S., Choi, N., and Kim, H.N. (2019) Brain-on-a-chip: a history of development and future perspective. *Biomicrofluidics* **13**: 51301.
- Bauer, A.W., Kirby, W.M.M., Sherris, J.C., and Turck, M. (1966) Antibiotic susceptibility testing by a standardized single disk method. *Am J Clin Pathol* **45**: 493–496.
- Bible, A.N., Fletcher, S.J., Pelletier, D.A., Schadt, C.W., Jawdy, S.S., Weston, D.J., *et al.* (2016) A carotenoid-deficient mutant in *Pantoea* sp. YR343, a bacteria isolated from the Rhizosphere of *Populus deltoides*, is defective in root colonization. *Front Microbiol* **7**: 1–15.
- Bodor, A., Bounedjoum, N., Vincze, G.E., Erdeiné Kis, Á., Laczi, K., Bende, G., *et al.* (2020) Challenges of unculturable bacteria: environmental perspectives. *Rev Environ Sci Biotechnol* **19**: 1–22.
- Cao, J., Nagl, S., Kothe, E., and Köhler, J.M. (2015) Oxygen sensor nanoparticles for monitoring bacterial growth and characterization of dose-response functions in microfluidic screenings. *Microchim Acta* **182**: 385–394.
- Caspi, Y. (2014) Deformation of filamentous *Escherichia coli* cells in a microfluidic device: a new technique to study cell mechanics. *PLoS One* **9**: e83775.
- Chang, C.B., Wilking, J.N., Kim, S.H., Shum, H.C., and Weitz, D.A. (2015) Monodisperse emulsion drop microenvironments for bacterial biofilm growth. *Small* **11**: 3954–3961.
- Chen, H., and De La Fuente, L. (2020) Calcium transcriptionally regulates movement, recombination and other functions of *Xylella fastidiosa* under constant flow inside microfluidic chambers. *Microb Biotechnol* **13**: 548–561.
- Cheng, S.Y., Heilman, S., Wasserman, M., Archer, S., Shuler, M.L., and Wu, M. (2007) A hydrogel-based microfluidic device for the studies of directed cell migration. *Lab Chip* **7**: 763–769.
- Cho, H.J., Jönsson, H., Campbell, K., Melke, P., Williams, J.W., Jedynak, B., *et al.* (2007) Self-organization in high-density bacterial colonies: efficient crowd control. *PLoS Biol* **5**: 2614–2623.
- Chong, Z.Z., Tan, S.H., Gañán-Calvo, A.M., Tor, S.B., Loh, N.H., and Nguyen, N.T. (2016) Active droplet generation in microfluidics. *Lab Chip* **16**: 35–58.
- Collins, D.J., Neild, A., deMello, A., Liu, A.Q., and Ai, Y. (2015) The Poisson distribution and beyond: Methods for microfluidic droplet production and single cell encapsulation. *Lab Chip* **15**: 3439–3459.
- Dangla, R., Gallaire, F., and Baroud, C.N. (2010) Microchannel deformations due to solvent-induced PDMS swelling. *Lab Chip* **10**: 2972–2978.
- Debré, P., and Le Gall, J.-Y. (2014) Le microbiote intestinal. *Bull Acad Natl Med* **198**: 1667–1684.
- Dehkharghani, A., Waisbord, N., Dunkel, J., and Guasto, J.S. (2019) Bacterial scattering in microfluidic crystal flows reveals giant active Taylor-Aris dispersion. *Proc Natl Acad Sci USA* **166**: 11119–11124.
- Demir, M., and Salman, H. (2012) Bacterial thermotaxis by speed modulation. *Biophys J* **103**: 1683–1690.
- Deng, Z.-S., Kong, Z.-Y., Zhang, B.-C., and Zhao, L.-F. (2020) Insights into non-symbiotic plant growth promotion bacteria associated with nodules of *Sphaerophysa salsula* growing in northwestern China. *Arch Microbiol* **202**: 399–409.
- Dong, L., Chen, D.W., Liu, S.J., and Du, W. (2016) Automated chemotactic sorting and single-cell cultivation of microbes using droplet microfluidics. *Sci Rep* **6**: 1–8.
- Durham, W.M., Tranzer, O., Leombruni, A., and Stocker, R. (2012) Division by fluid incision: Biofilm patch development in porous media. *Phys Fluids* **24**: 91107.

- Englert, D.L., Manson, M.D., and Jayaraman, A. (2009) Flow-based microfluidic device for quantifying bacterial chemotaxis in stable, competing gradients. *Appl Environ Microbiol* **75**: 4557–4564.
- Friend, J., and Yeo, L. (2010) Fabrication of microfluidic devices using polydimethylsiloxane. *Biomicrofluidics* **4**: 1–5.
- Gökaltun, A., Kang, Y.B. (Abraham), Yarmush, M.L., Usta, O.B., and Asatekin, A. (2019) Simple surface modification of Poly(dimethylsiloxane) via surface segregating smart polymers for biomicrofluidics. *Sci Rep* **9**: 1–14.
- Golchin, S.A., Stratford, J., Curry, R.J., and McFadden, J. (2012) A microfluidic system for long-term time-lapse microscopy studies of mycobacteria. *Tuberculosis* **92**: 489–496.
- Haldorsson, S., Lucumi, E., Gómez-Sjöberg, R., and Fleming, R.M.T. (2015) Advantages and challenges of microfluidic cell culture in polydimethylsiloxane devices. *Biosens Bioelectron* **63**: 218–231.
- Hansen, R.H., Timm, A.C., Timm, C.M., Bible, A.N., Morrell-Falvey, J.L., Pelletier, D.A., et al. (2016) Stochastic assembly of bacteria in microwell arrays reveals the importance of confinement in community development. *PLoS One* **11**: 1–18.
- Harmon, J.B., Gray, H.K., Young, C.C., and Schwab, K.J. (2020) Microfluidic droplet application for bacterial surveillance in fresh-cut produce wash waters. *PLoS One* **15**: 1–24.
- Henriques-Normark, B., and Normark, S. (2014) Bacterial vaccines and antibiotic resistance. *Ups J Med Sci* **119**: 205–208.
- Ho, C.T., Lin, R.Z., Chang, W.Y., Chang, H.Y., and Liu, C.H. (2006) Rapid heterogeneous liver-cell on-chip patterning via the enhanced field-induced dielectrophoresis trap. *Lab Chip* **6**: 724–734.
- Ho, C.M.B., Sun, Q., Teo, A.J.T., Wibowo, D., Gao, Y., Zhou, J., et al. (2020) Development of a microfluidic droplet-based microreactor for microbial cultivation. *ACS Biomater Sci Eng* **6**: 3630–3637.
- Hosokawa, M., Nishikawa, Y., Kogawa, M., and Takeyama, H. (2017) Massively parallel whole genome amplification for single-cell sequencing using droplet microfluidics. *Sci Rep* **7**: 3–4.
- Houpikian, P., and Raoult, D. (2002) Traditional and molecular techniques for the study of emerging bacterial diseases: one laboratory's perspective. *Emerg Infect Dis* **8**: 122–131.
- Huang, M., Fan, S., Xing, W., and Liu, C. (2010) Microfluidic cell culture system studies and computational fluid dynamics. *Math Comput Model* **52**: 2036–2042.
- Huh, D. (2015) A human breathing lung-on-a-chip. *Ann Am Thorac Soc* **12**: S42–S44.
- Hyun, J.K., Boedicker, J.Q., Jang, W.C., and Ismagilov, R.F. (2008) Defined spatial structure stabilizes a synthetic multispecies bacterial community. *Proc Natl Acad Sci USA* **105**: 18188–18193.
- Ishikawa, T., Shioiri, T., Numayama-Tsuruta, K., Ueno, H., Imaia, Y., and Yamaguchi, T. (2014) Separation of motile bacteria using drift velocity in a microchannel. *Lab Chip* **14**: 1023–1032.
- Ito, T., Sekizuka, T., Kishi, N., Yamashita, A., and Kuroda, M. (2019) Conventional culture methods with commercially available media unveil the presence of novel culturable bacteria. *Gut Microbes* **10**: 77–91.
- Jeong, H.H., Jeong, S.G., Park, A., Jang, S.C., Hong, S.G., and Lee, C.S. (2014) Effect of temperature on biofilm formation by Antarctic marine bacteria in a microfluidic device. *Anal Biochem* **446**: 90–95.
- Jin, Z., Nie, M., Hu, R., Zhao, T., Xu, J., Chen, D., et al. (2018) Dynamic sessile-droplet habitats for controllable cultivation of bacterial biofilm. *Small* **14**: 1–8.
- Johnson, D. (2018) Bacterial Pathogens and Their Virulence Factors. Cham, Switzerland: Springer International Publishing.
- Julich, S., Hotzel, H., Gärtner, C., Trouchet, D., El Metwaly, F., Ahmed, M., et al. (2016) Evaluation of a microfluidic chip system for preparation of bacterial DNA from swabs, air, and surface water samples. *Biologicals* **44**: 574–580.
- Kaminski, T.S., Scheler, O., and Garstecki, P. (2016) Droplet microfluidics for microbiology: Techniques, applications and challenges. *Lab Chip* **16**: 2168–2187.
- Kaushik, A.M., Hsieh, K., Chena, L., Shina, D.J., Liaob, J.C., and Wang, T.-H. (2017) Accelerating bacterial growth detection and antimicrobial susceptibility assessment in integrated picoliter droplet platform. *Biosens Bioelectron* **97**: 260–266.
- Kaya, T., and Koser, H. (2012) Direct upstream motility in *Escherichia coli*. *Biophys J* **102**: 1514–1523.
- Kibret, M., and Abera, B. (2011) Antimicrobial susceptibility patterns of *E. coli* from clinical sources in northeast Ethiopia. *Afr Health Sci* **11**: S40–S45.
- Kim, B.J., Chu, I., Jusuf, S., Kuo, T., TerAvest, M.A., Angent, L.T., and Wu, M. (2016) Oxygen tension and riboflavin gradients cooperatively regulate the migration of *Shewanella oneidensis* MR-1 revealed by a hydrogel-based microfluidic device. *Front Microbiol* **7**: 1–12.
- Kim, H.J., and Ingber, D.E. (2013) Gut-on-a-Chip microenvironment induces human intestinal cells to undergo villus differentiation. *Integr Biol* **5**: 1130–1140.
- Kim, S., Lee, S., Kim, J.K., Chung, H.J., and Jeon, J.S. (2019) Microfluidic-based observation of local bacterial density under antimicrobial concentration gradient for rapid antibiotic susceptibility testing. *Biomicrofluidics* **13**: 14108.
- Krell, T., Lacal, J., Muñoz-Martínez, F., Reyes-Darias, J.A., Cadirci, B.H., García-Fontana, C., and Ramos, J.L. (2011) Diversity at its best: bacterial taxis. *Environ Microbiol* **13**: 1115–1124.
- Kudva, I.T., Cornick, N.A., Plummer, P.J., Zhang, Q., Nicholson, T.L., Bannantine, J.P., and Bellaire, B.H. (2016) *Virulence Mechanisms of Bacterial Pathogens* (5th edn.). Washington, DC: ASM books.
- Lam, R.H.W., Kim, M.C., and Thorsen, T. (2009) Culturing aerobic and anaerobic bacteria and mammalian cells with a microfluidic differential oxygenator. *Anal Chem* **81**: 5918–5924.
- Lambert, G., and Kussel, E. (2014) Memory and fitness optimization of bacteria under fluctuating environments. *PLoS Genet* **10**: e1004556.
- Lamouche, F., Gully, D., Chaumeret, A., Nouwen, N., Verly, C., Pierre, O., et al. (2018) Transcriptomic dissection of *Bradyrhizobium* sp. strain ORS285 in symbiosis with *Aeschynomene* spp. inducing different bacteroid

- morphotypes with contrasted symbiotic efficiency. *Environ Microbiol* **21**, 3244–3258.
- Lanning, L.M., Ford, R.M., and Long, T. (2008) Bacterial chemotaxis transverse to axial flow in a microfluidic channel. *Biotechnol Bioeng* **100**: 653–663.
- Lashkaripour, A., Rodriguez, C., Ortiz, L., and Densmore, D. (2019) Performance tuning of microfluidic flow-focusing droplet generators. *Lab Chip* **19**: 1041–1053.
- Lebeaux, D., Chauhan, A., Rendueles, O., and Beloin, C. (2013) From in vitro to in vivo models of bacterial biofilm-related infections. *Pathogens* **2**: 288–356.
- Li, H., Torab, P., Mach, K.E., Surette, C., England, M.R., Craft, D.W., *et al.* (2019) Adaptable microfluidic system for single-cell pathogen classification and antimicrobial susceptibility testing. *Proc Natl Acad Sci USA* **116**: 10270–10279.
- Liberman, L., Berg, H.C., and Sourjik, V. (2004) Effect of chemoreceptor modification on assembly and activity of the receptor-kinase complex in *Escherichia coli*. *J Bacteriol* **186**: 6643–6646.
- Long, T., and Ford, R.M. (2009) Enhanced transverse migration of bacteria by chemotaxis in a porous T-sensor. *Environ Sci Technol* **43**: 1546–1552.
- Lukic, J., Chen, V., Strahinic, I., Begovic, J., Lev-Tov, H., Davis, S.C., *et al.* (2017) Probiotics or pro-healers the role of beneficial bacteria in tissue repair. *Wound Repair Regen* **25**: 912–922.
- Mahler, L., Niehs, S., Martin, K., Weber, T., Scherlach, K., Agler-Rosenbaum, M., *et al.* (2019) Highly parallelized microfluidic droplet cultivation and prioritization on antibiotic producers from complex natural microbial communities. *bioRxiv*. Doi: 10.1101/2019.12.18.877530
- Mahler, L., Tovar, M., Weber, T., Brandes, S., Rudolph, M.M., Ehgartner, J., *et al.* (2015) Enhanced and homogeneous oxygen availability during incubation of microfluidic droplets. *RSC Adv* **5**: 101871–101878.
- Mao, H., Cremer, P.S., and Manson, M.D. (2003) A sensitive, versatile microfluidic assay for bacterial chemotaxis. *Proc Natl Acad Sci USA* **100**: 5449–5454.
- Marcos, Fu, H.C., Powers, T.R., and Stocker, R. (2009) Separation of microscale chiral objects by shear flow. *Phys Rev Lett* **102**: 158103.
- Marty, A., Causserand, C., Roques, C., and Bacchin, P. (2014) Impact of tortuous flow on bacteria streamer development in microfluidic system during filtration. *Biomicrofluidics* **8**: 14105.
- Mathai, P.P., Dunn, H.M., Venkiteshwaran, K., Zitomer, D.H., Maki, J.S., Ishii, S., and Sadowsky, M.J. (2019) A microfluidic platform for the simultaneous quantification of methanogen populations in anaerobic digestion processes. *Environ Microbiol* **21**: 1798–1808.
- Matsumoto, Y., Sakakihara, S., Grushnikov, A., Kikuchi, K., Noji, H., Yamaguchi, A., *et al.* (2016) A microfluidic channel method for rapid drug-susceptibility testing of *Pseudomonas aeruginosa*. *PLoS One* **11**: 1–17.
- van Meer, B.J., de Vries, H., Firth, K.S.A., van Weerd, J., Tertoolen, L.G.J., Karperien, H.B.J., *et al.* (2017) Small molecule absorption by PDMS in the context of drug response bioassays. *Biochem Biophys Res Commun* **482**: 323–328.
- Menolascina, F., Rusconi, R., Fernandez, V.I., Smriga, S., Aminzare, Z., Sontag, E.D., and Stocker, R. (2017) Logarithmic sensing in *Bacillus subtilis* aerotaxis. *npj Syst Biol Appl* **3**: 36.
- Mesibov, R., and Adler, J. (1972) Chemotaxis toward amino acids in *Escherichia coli*. *J Bacteriol* **112**: 315–326.
- Miller, S., Weiss, A.A., Heineman, W.R., and Banerjee, R.K. (2019) Electroosmotic flow driven microfluidic device for bacteria isolation using magnetic microbeads. *Sci Rep* **9**: 1–11.
- Mirzaei, R., Mohammadzadeh, R., Sholeh, M., Karampoor, S., Abdi, M., Dogan, E., *et al.* (2020) The importance of intracellular bacterial biofilm in infectious diseases. *Microb Pathog* **147**: 104393.
- Murugesan, N., Dhar, P., Panda, T., and Das, S.K. (2017) Interplay of chemical and thermal gradient on bacterial migration in a diffusive microfluidic device. *Biomicrofluidics* **11**: 1–13.
- Myklatun, A., Cappetta, M., Winklhofer, M., Ntziachristos, V., and Westmeyer, G.G. (2017) Microfluidic sorting of intrinsically magnetic cells under visual control. *Sci Rep* **7**: 1–8.
- Oblath, E.A., Henley, W.H., Alarie, J.P., and Ramsey, J.M. (2013) A microfluidic chip integrating DNA extraction and real-time PCR for the detection of bacteria in saliva. *Lab Chip* **13**: 1325–1332.
- Ota, Y., Saito, K., Takagi, T., Matsukura, S., Morita, M., Tsuneda, S., and Noda, N. (2019) Fluorescent nucleic acid probe in droplets for bacterial sorting (FNAP-sort) as a high-throughput screening method for environmental bacteria with various growth rates. *PLoS One* **14**: 1–18.
- Overmann, J., Abt, B., and Sikorski, J. (2017) Present and future of culturing bacteria. *Annu Rev Microbiol* **71**: 711–730.
- Partridge, J.D., Nhu, N.T.Q., Dufour, Y.S., and Harshey, R.M. (2019) *Escherichia coli* remodels the chemotaxis pathway for swarming. *MBio* **10**: 1–16.
- Parvinzadeh Gashti, M., Asselin, J., Barbeau, J., Boudreau, D., and Greener, J. (2016) A microfluidic platform with pH imaging for chemical and hydrodynamic stimulation of intact oral biofilms. *Lab Chip* **16**: 1412–1419.
- Paulick, A., Jakovljevic, V., Zhang, S., Erickstad, M., Groisman, A., Meir, Y., *et al.* (2017) Mechanism of bidirectional thermotaxis in *Escherichia coli*. *eLife* **6**: 26607.
- Phillips, K.N., Castillo, G., Wünsche, A., and Cooper, T.F. (2016) Adaptation of *Escherichia coli* to glucose promotes evolvability in lactose. *Evolution* **70**: 465–470.
- Polacheck, W.J., Kutys, M.L., Tefft, J.B., and Chen, C.S. (2019) *Microfabricated Blood Vessels for Modeling the Vascular Transport Barrier*. Springer US.
- Pratt, S.L., Zath, G.K., Akiyama, T., Williamson, K.S., Franklin, M.J., and Chang, C.B. (2019) DropSOAC: Stabilizing microfluidic drops for time-lapse quantification of single-cell bacterial physiology. *Front Microbiol* **10**: 1–13.
- Rath, H., Stumpp, N., and Stiesch, M. (2017) Development of a flow chamber system for the reproducible in vitro analysis of biofilm formation on implant materials. *PLoS One* **12**: 1–12.
- Rismani Yazdi, S., Nosrati, R., Stevens, C.A., Vogel, D., and Escobedo, C. (2018a) Migration of magnetotactic bacteria in porous media. *Biomicrofluidics* **12**: 11101.
- Rismani Yazdi, S., Nosrati, R., Stevens, C.A., Vogel, D., Davies, P.L., and Escobedo, C. (2018b) Magnetotaxis

- enables magnetotactic bacteria to navigate in flow. *Small* **14**: 1–10.
- Roggo, C., Picioareanu, C., Richard, X., Mazza, C., van Lin-
tel, H., and van der Meer, J.R. (2018) Quantitative chemical biosensing by bacterial chemotaxis in microfluidic chips. *Environ Microbiol* **20**: 241–258.
- Rusconi, R., Lecuyer, S., Guglielmini, L., and Stone, H.A. (2010) Laminar flow around corners triggers the formation of biofilm streamers. *J R Soc Interface* **7**: 1293–1299.
- Sackmann, E.K., Fulton, A.L., and Beebe, D.J. (2014) The present and future role of microfluidics in biomedical research. *Nature* **507**: 181–189.
- Salman, H., Zilman, A., Loverdo, C., Jeffroy, M., and Libchaber, A. (2006) Solitary modes of bacterial culture in a temperature gradient. *Phys Rev Lett* **97**: 1–5.
- Schilling, E.A., Kamholz, A.E., and Yager, P. (2002) Cell lysis and protein extraction in a microfluidic device with detection by a fluorogenic enzyme assay. *Anal Chem* **74**: 1798–1804.
- Segall, J.E., Manson, M.D., and Berg, H.C. (1982) Signal processing times in bacterial chemotaxis. *Nature* **296**: 855–857.
- Shin, S., Kim, N., and Hong, J.W. (2018) Comparison of surface modification techniques on polydimethylsiloxane to prevent protein adsorption. *Biochip J* **12**: 123–127.
- Shin, Y., Han, S., Jeon, J.S., Yamamoto, K., Zervantonakis, I.K., Sudo, R., *et al.* (2012) Microfluidic assay for simultaneous culture of multiple cell types on surfaces or within hydrogels. *Nat Protoc* **7**: 1247–1259.
- Simmons, E.L., Bond, M.C., Koskella, B., Drescher, K., Bucci, V., and Nadella, C.D. (2020) Biofilm structure promotes coexistence of phage-resistant and phage-susceptible bacteria. *mSystems* **5**: 1–17.
- Stricker, L., Guido, I., Breithaupt, T., Mazza, M.G., and Vollmer, J. (2019) Hybrid sideways/longitudinal swimming in the monoflagellate *Shewanella oneidensis*: from aerotactic band to biofilm. Physics (College Park Md).
- Subramanian, S., Huiszoon, R.C., Chu, S., Bentley, W.E., and Ghodssi, R. (2020) Microsystems for biofilm characterization and sensing – a review. *Biofilm* **2**: 100015.
- Takeuchi, S., DiLuzio, W.R., Weibel, D.B., and Whitesides, G.M. (2005) Controlling the shape of filamentous cells of *Escherichia Coli*. *Nano Lett* **5**: 1819–1823.
- Thacker, V.V., Dhar, N., Sharma, K., Barrile, R., Karalis, K., and McKinney, J.D. (2020) A lung-on-chip model of early *M. tuberculosis* infection reveals an essential role for alveolar epithelial cells in controlling bacterial growth. *eLife* **9**: 1–22.
- Velve-Casquillas, G., Le Berre, M., Piel, M., and Tran, P.T. (2010) Microfluidic tools for cell biological research. *Nano Today* **5**: 28–47.
- Vinderola, G., Gueimonde, M., Gomez-Gallego, C., Delfederico, L., and Salminen, S. (2017) Correlation between in vitro and in vivo assays in selection of probiotics from traditional species of bacteria. *Trends Food Sci Technol* **68**: 83–90.
- Vives-Peris, V., de Ollas, C., Gómez-Cadenas, A., and Pérez-Clemente, R.M. (2020) Root exudates: from plant to rhizosphere and beyond. *Plant Cell Rep* **39**: 3–17.
- Wang, P., Robert, L., Pelletier, J., Dang, W.L., Taddei, F., Wright, A., and Jun, S. (2010) Robust growth of *Escherichia coli*. *Curr Biol* **20**: 1099–1103.
- Watterson, W.J., Tanyeri, M., Watson, A.R., Cham, C.M., Shan, Y., Chang, E.B., *et al.* (2020) Droplet-based high-throughput cultivation for accurate screening of antibiotic resistant gut microbes. *eLife* **9**: 1–22.
- Weibel, D.B., DiLuzio, W.R., and Whitesides, G.M. (2007) Microfabrication meets microbiology. *Nat Rev Microbiol* **5**: 209–218.
- White, A.R., Jalali, M., and Sheng, J. (2019) A new ecology-on-a-chip microfluidic platform to study interactions of microbes with a rising oil droplet. *Sci Rep* **9**: 1–11.
- Wolfe, A.J., and Berg, H.C. (1989) Migration of bacteria in semisolid agar. *Proc Natl Acad Sci USA* **86**: 6973–6977.
- Wright, E., Neethirajan, S., Warriner, K., Retterer, S., and Srijanto, B. (2014) Single cell swimming dynamics of *Listeria monocytogenes* using a nanoporous microfluidic platform. *Lab Chip* **14**: 938–946.
- Yazdi, S., and Ardekani, A.M. (2012) Bacterial aggregation and biofilm formation in a vortical flow. *Biomicrofluidics* **6**: 44114.
- You, J.B., Lee, B., Choi, Y., Lee, C.S., Peter, M., Im, S.G., and Lee, S.S. (2020) Nanoadhesive layer to prevent protein absorption in a poly(dimethylsiloxane) microfluidic device. *Biotechniques* **69**: 47–52.
- Zhang, X.Y., Sun, K., Abulimiti, A., Xu, P.P., and Li, Z.Y. (2019) Microfluidic system for observation of bacterial culture and effects on biofilm formation at microscale. *Micro-machines* **10**: 606.
- Zhuang, J., Carlsen, R.W., and Sitti, M. (2015) PH-taxis of biohybrid microsystems. *Sci Rep* **5**: 11403.